

Reponse to Interactive comment on “Reassessing the ratio of glyoxal to formaldehyde as an indicator of hydrocarbon precursor speciation” by J. Kaiser et al.

Anonymous Referee #1

We thank the referee for the valuable comments. The original comments are shown in italicized black, while responses are provided below in blue.

The conclusion that the updated OMI CHOCHO data can provide better agreement between satellite and in-situ R_{GF} observations is based on the comparison between the 2007 OMI data to the 2013 in-situ data. However, the time difference between the two datasets is so large that many things (e.g., VOC emissions, NO_x levels, oxidation capacity / OH level) can change during the long time period. These changes could result in different concentrations and spatial distributions of HCHO and CHOCHO in 2013 than in 2007. Consequently, R_{GF} may not be the same in the two years. If it is possible, I strongly suggest the authors to use 2013 OMI data for this manuscript. Otherwise, the authors should explicitly explain why the R_{GF} derived from OMI observations are similar in the summer of 2007 and 2013. A figure illustrating the change of emission patterns of AVOCs, BVOCs, NO_x , CO, etc. would be helpful.

While ideally 2013 OMI retrievals would be used in this analysis, the satellite has experienced severe degradation such that quantitative CHOCHO is not easily determined. Only the 2007 retrievals are available at this time. One of the major conclusions reached using the SENEX measurements is that in the SE US, R_{GF} is not a diagnostic of anthropogenic emissions, as HCHO and CHOCHO production are dominated by isoprene oxidation. Our in-situ measurements also show that R_{GF} is unaffected by NO_x and OH (section 3.3). Therefore, as long as isoprene is the dominant VOC for HCHO and CHOCHO production in the SE US in both 2007 and 2013, the comparison between 2007 satellite and 2013 in-situ R_{GF} remains valid. Both this work and analysis of the previous 1995 Nashville/Middle Tennessee Ozone Study (Le et al., 1998) find isoprene to be the dominant HCHO source. Interannual variability of summertime isoprene emissions is estimated to be between 8 and 18% for the contiguous U.S. during the summers (Tawfik et al., 2012). Therefore, it is likely that isoprene is also the dominant OVOC source in 2007.

This discussion is now included in section 3.5 (comparison with satellite retrievals).

Specific comments

Line 6, Page 6239: “the oxidation products” → “HCHO and CHOCHO”.

Corrected.

Line 17–19: This conclusion is valid only if the points described in the general comments have been addressed.

We have now addressed this comment in section 3.5.

Line 19 – 21, Page 6239: I think rationale behind this conclusion is not well explained in the manuscript. What kind of other measurements are needed? How can the diagnostic by R_{GF} been improved by these measurements?

A more careful conclusion is stated: "... [W]e conclude that satellite-based observations of R_{GF} can be used alongside knowledge of land-use as a global diagnostic of dominant hydrocarbon speciation."

Line 14, Page 6240: Do alkenes include isoprene and monoterpenes? Probably it is better to use "particularly alkenes, aromatics, isoprene, and monoterpenes".

We now use this suggested clarification.

Line 3, Page 6242: "CHOCHO vcds" → "CHOCHO vertical column densities (Ω_V)." To avoid any confusion, I suggest to use the same symbol for vertical column density as that used in satellite retrievals.

We now consistently refer to vertical column densities using the symbol Ω_V .

Line 7, Page 6244: "slant columns (Ω_S)" → "slant column densities (Ω_S)."

Corrected.

Line 10, Page 6244: "vertical columns (Ω_S)" → "vertical column densities (Ω_V)."

Corrected.

Section 2.2, Page 6244: Please add description on the time period of the OMI data used in this study. It should also mention that the used OMI data are averaged data over this time period.

We now include in section 2.2 that we use the average vertical column densities for June through August of 2007.

Line 5, Page 6245: I understand that the term OVOC in this manuscript only refers to HCHO and / or CHOCHO. Since the normally used OVOC contains more species, the authors should make a clear statement on the species included in their defined OVOC.

We now clarify that we are referring specifically to HCHO and CHOCHO. Throughout the manuscript, we either refer to "both OVOCs" or "HCHO and CHOCHO" rather than using the more broad term "OVOCs".

Line 7, Page 6245: Can the authors mark the "isoprene volcano" in Figure 1?

The Ozarks are labeled in the top panel of Figure 1.

Line 8, Page 6245: What does the “background” refer to? Does it mean regions dominated by BVOC emissions? I suggest to reformat this sentence so that the meaning of “background” is clearer.

We have reworded this to state that the concentrations of both OVOCs are higher in regions with anthropogenic influence than in the surrounding biogenically dominated areas.

Line 9 – 10, Page 6245: I suggest to mark the location of these cities in Figure 1, so that the outflows of the city can be easily identified.

These cities are labeled in the top panel of Figure 1.

Line 22–24, Page 6245: This sentence is difficult to understand. For comparison between observations in different days, the effect of diurnal variation can be minimized by using data obtained at similar time of the day. However, for observations in an individual day, how to minimize this effect?

We have reworded our explanation to state: “By comparing the observations made within 1 hour on the same day, we aim to minimize any impact diurnal variation of R_{GF} would have on this analysis.”

There are four flights for which we compare R_{GF} measured at one location to another location on the same flight. On the June 12th flight, all measurements used in the in-and-out of plume comparisons are acquired over ~1.5 hrs (Fig 7). Both in-plume and background regions are sampled multiple times, and neither show a temporal trend in R_{GF} over the time span of the observations. On both the June 10th and June 25th flights, we highlight the southeast corner of the flight track as a region of high R_{GF}. The time elapsed between measuring the observations at the southeast corner of the flight track and the northwest region of the flight track is ~1 hr. Finally, on the 26 June flight, we highlight the Ozarks as a region of low R_{GF}. The R_{GF} is low compared to the southwest portion of the flight path, which was sampled approximately 3 hours before the measurements over the Ozarks. This amount of time is considerably longer than the maximum times between measurements used in the comparisons for the other flights. For that reason, we have included it as a possible reason for the observed differences in R_{GF} in section 3.2.

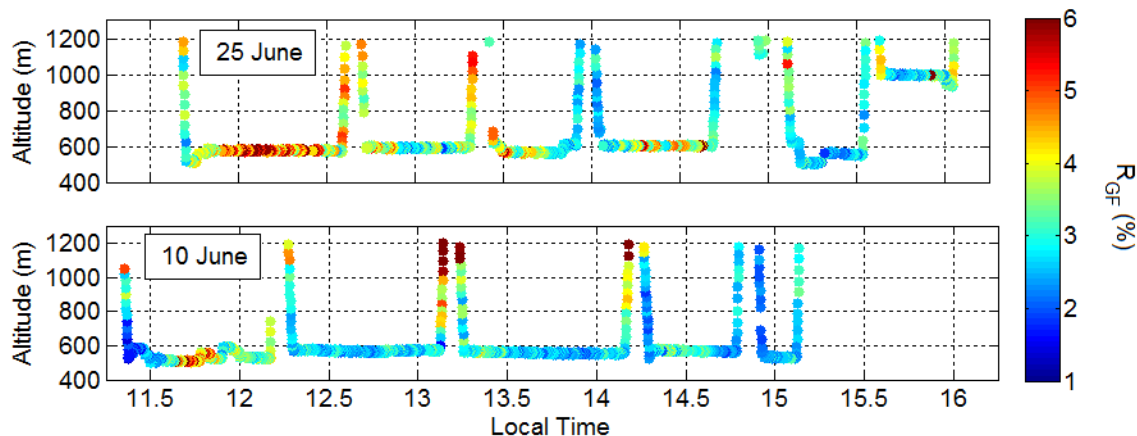
Line 26, Page 6245: “On both the 10 June and 25th flights,” → “During flights on both 10 June and 25 June,”.

Corrected.

Line 10 – 20, Page 6246: The R_{GF} on 25 June is in general higher than that on 10 June. Is this difference also caused by the incursion of air mass from free troposphere? In a later section, the authors described that R_{GF} changes with altitude. Therefore, I think it is also worth to mention, on 10 and 25 June, whether the R_{GF} for a certain location is obtained at similar flight altitude.

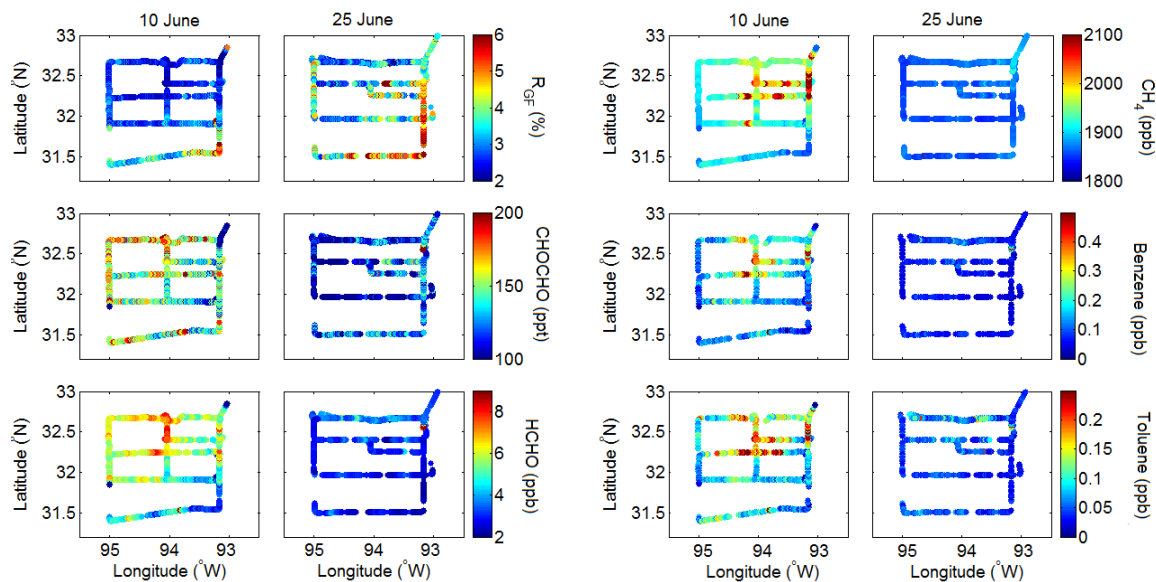
The incursion of the free tropospheric air mass appears limited to the region circled in Figure 3, as shown in Figure 5.

The figure below is a time series of altitude colored by R_{GF} for each flight. The primary flying altitude for both flights is ~ 600 m. The difference in R_{GF} between the two flights does not appear to be altitude driven.



While R_{GF} is typically slightly higher in the free troposphere than the boundary layer, no clear altitude dependence in R_{GF} is observed within the boundary layer (Figure 8c, altitudes less than 2 km, and figure S4 for individual profiles). Therefore, as long as measurements are acquired in the boundary layer, altitude should have little effect on R_{GF} . This is now explained further in section 3.5. Because all flight tracks remain primarily within the boundary layer, this negates the need of showing altitude measurements along the flight track.

Another possibility for the differences in R_{GF} observed on the two days is the emission strength of the underlying VOCs. As shown below, both CHOCHO and HCHO concentrations are higher on 10 June, while R_{GF} is lower. On 10 June, concentrations of anthropogenic VOCs (e.g. CH_4 , benzene, and toluene) are higher. It is possible that the CHOCHO and HCHO budgets are more influenced by these AVOCs on 10 June, such that the influence of monoterpene emissions on R_{GF} is stronger on 25 June. However, this discussion is beyond the intent of our comparison, which is to compare only measurements acquired on the same flight.



Line 22, Page 6246: Please specify the major wind direction before using the term upwind.

We have eliminated the term upwind to avoid confusion.

Line 24 – 25, Page 6246: Which type of VOC is dominant in terms of OH reactivity? BVOC or AVOC?

Of the measured VOCs, isoprene constitutes the majority (74%) of the total OH reactivity of the measured primary VOCs for this subset of measurements. This excludes HCHO, CHOCHO, and CH₃CHO, which contribute significantly to the calculated OH reactivity. This is now mentioned in this paragraph.

Line 25, Page 6246: CO₂ data is not shown in Figure 4.

For simplicity, rather than including a 5th subplot, we will not refer to CO₂ measurements. CH₄ measurements (subfigure f) fully illustrate the emissions associated with oil and natural gas production.

Line 9 – 11, Page 6247: Please add the specific references. As far as I can see, not all literatures in Table 1 support this argument.

The references that specifically discuss ozone production are now listed.

Line 11 – 14, Page 6247: To be consistent with the occurrence in the following text, I suggest to exchange position of the second and the third explanation.

Corrected.

Line 6, Page 6248: Can the authors provide a measurement evidence supporting “isoprene is still likely the dominant OVOC precursor”? E.g., the contribution of isoprene to the total OH reactivity of the measured VOCs.

We now state that the contribution of isoprene and its first generation oxidation products methyl-vinyl-ketone (MVK) and methacrolein (MACR) to OH reactivity is more than a factor of 10 times greater than the contribution from measured AVOCs.

Line 20 – 23, Page 6248: Is this because the production of HCHO and CHOCHO from isoprene oxidation is less sensitive to the change of NO_x concentrations?

Though the low-NO_x isoprene oxidation mechanism is still unknown, most modeling studies agree that both CHOCHO and HCHO yields are sensitive to NO_x concentrations, with lower yields at lower NO (i.e. Marais et al. 2012; Fu et al. 2008). Our results suggest that the two oxidation products are effected in a similar manner such that R_{GF} is unaffected by RO₂ fate, or that the influence of NO is counterbalanced by competing influences on R_{GF} within the plume.

Line 26, Page 6248: Ozarks is not explicitly mentioned in Section 3.2.

We now explicitly state the Mark Twain National Forest is in the Missouri Ozarks.

Line 4–6, Page 6251: Change to “a convoluted diagnostic for assessing the VOC compositions”. Because there is no evidence supporting the link between RGF and ozone formation.

We agree with the reviewer, and have changed the wording accordingly.

Line 9 – 12, Page 6251: Why should the point measurements represent the monthly mean values? OMI or GOME can provide VCDs on daily base.

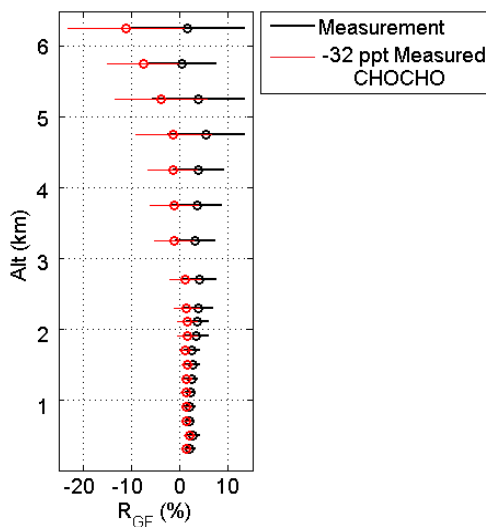
The phrase “monthly mean” is now replaced with “seasonal mean”. The comparison between point and satellite values is performed on seasonally-averaged satellite data for two reasons: (1) we are reassessing the previous comparisons performed in literature, which used seasonal averages at best (though multi-year averages are also used). (2) given the error in satellite measurements, seasonal averaging is necessary to arrive at meaningful trends in regional R_{GF}.

Line 12, Page 6251: What does the “vertical structure” refer to?

We’ve reworded this section to explicitly refer to the vertical distribution of HCHO and CHOCHO.

Line 22 – 23, Page 6251: Why there could be a positive bias in CHOCHO measurements? The authors should mention this point in Section 2.1.

The potential bias we discuss is within the measurement uncertainty. The ACES instrument precision (32 ppt) is



limited by shot noise. The accuracy (6%) is limited by knowledge of Rayleigh scattering cross sections, absorption cross sections, and sample pressure and temperature. Because the uncertainty in CHOCHO concentrations from measurement precision is greater than that from measurement accuracy, we take (Measured CHOCHO – 32 ppt) as the lower limit of CHOCHO as measured by ACES. We have reworded this section to be clear that by addressing a possible bias, we are in fact addressing the measurement uncertainty, which is discussed in greater detail in Washenfelder et al. (2011). It is unclear if any bias in CHOCHO measurements exists; however, this would change the altitude dependence of R_{GF} (see figure to right).

Line 25 – 28, Page 6251: Compared to HCHO, CHOCHO is usually produced as third or fourth generation product of isoprene oxidation (c.f., MCMv3.2). Could this also cause the difference in vertical distribution between HCHO and CHOCHO?

Li et al. (2014) found different mixing layer heights for the two OVOCs. They calculated that the lifetime of isoprene was shorter than the typical boundary layer mixing time, and therefore hypothesized that HCHO production happened earlier (i.e. at lower altitudes) than CHOCHO production, in agreement with the reviewer’s hypothesis.

In contrast, we see that the boundary layer is typically uniformly mixed with respect to HCHO and CHOCHO, such that the two OVOCs have the same mixing height and R_{GF} is constant in the boundary layer (Figure 8c, altitudes less than 2 km, and Figure S4 for individual profiles). Therefore, the time dependence of HCHO and CHOCHO production is unlikely to be the underlying cause of the difference in R_{GF} observed in the free troposphere. This can be partly explained because the profile of HCHO and CHOCHO does not only depend on production from isoprene but because the lifetimes of these two, which is longer than that of isoprene.

The second reviewer comments that heterogeneous oxidation of aerosols might release glyoxal and other OVOCs in the free troposphere (Volkamer et al., 2015), and that the heterogeneous ozonolysis of fatty acids has indeed been found to be a source of glyoxal and other compounds (Zhou et al., 2014). These discussion points are now included in section 3.5.

Line 6, Page 6252: The term “column-integrated R_{GF} ” is confusing. It reads like the sum up of R_{GF} over the entire vertical column. I think what the authors meant should be the R_{GF} calculated from tropospheric VCDs.

The reviewer is correct in their interpretation of “column-integrated R_{GF} ”, though the term could be a source of confusion. We have reworded this section for clarity.

Line 20, Page 6252: Isn’t it 2007 instead of 2006?

Corrected.

Line 2, Page 6253: “column vcds” → “vertical column densities”.

Corrected.

Line 21, Page 6253: Please add references for “previous studies”.

Corrected.

Line 25 – 27, Page 6253: Can you see the difference between annual averages and monthly averages from your own OMI data in 2007?

Below we show HCHO and CHOCHO vertical column densities from OMI averaged over June through August 2007 (left), and over the entire year (right). The spatial distribution of HCHO appears similar in the summer and the annual averages, likely because the high summer concentrations dominant the yearly averages. In the glyoxal averages, summertime measurements show hotspots not seen in the annual averages. This difference in spatial patterns translates to different spatial patterns in observed R_{GF} both globally and over the US.

We do not see the hypothesized lower R_{GF} in the summer compared to the annual average over isoprene dominated regions (bottom panel, ocean data not shown for clarity). However, large differences are seen in other areas, such as the boreal forests, where monoterpene emissions are high. Therefore, we keep the hypothesis that point-based measurements may be biased to display the influence of BVOC emissions on R_{GF} , but remove the example of isoprene.

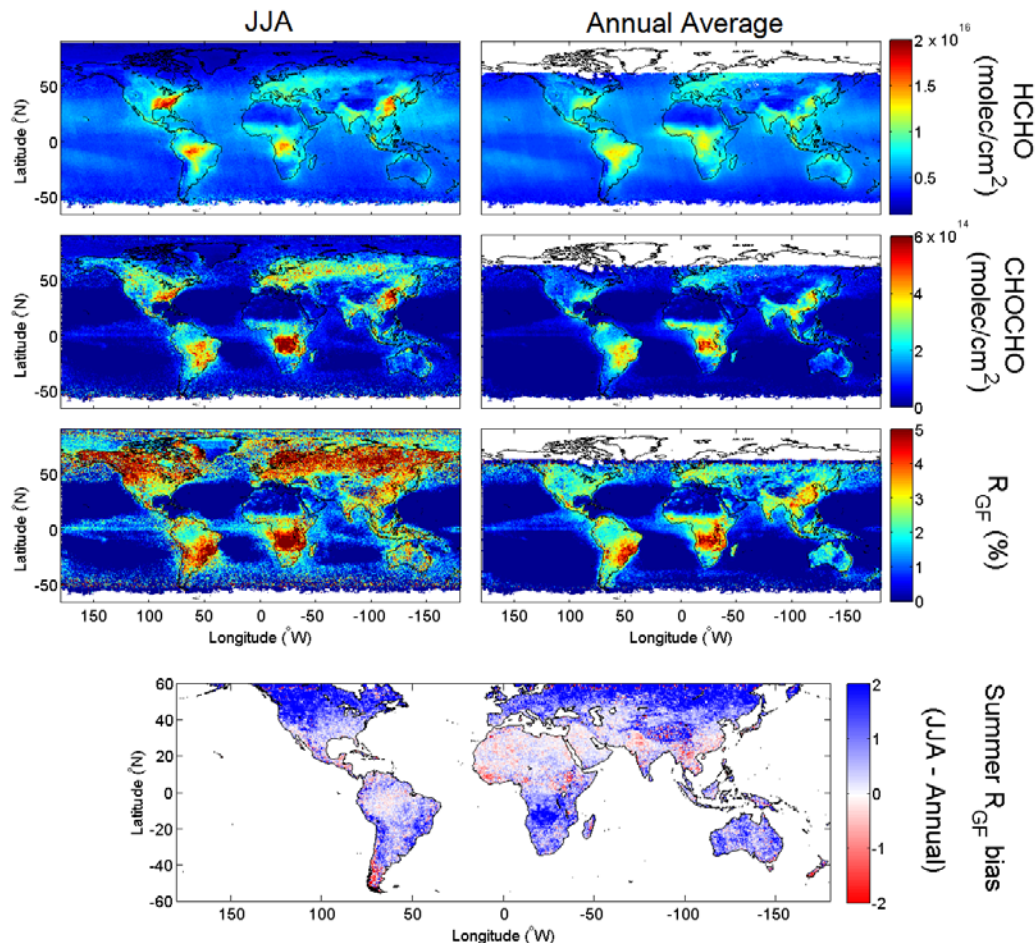


Table 3: Please describe the acronym FT in the footnote c.

F.T. (free troposphere) is now defined in the footnote.

Table 4: In footnote b, what about the calculation for HCHO mixing ratio?

We now clarify that both CHOCHO and HCHO are calculated in the same manner.

Figure 1: I suggest to change the symbol colors of power plant well, so that the individual points can be easily seen. The same for other similar figures in the manuscript.

The symbol colors have been changed.

Figure 2: For pints below the 1% line, are they related with direct emissions of HCHO?

These points are discussed in section 3.2 and shown in Figure 4. Direct emissions of HCHO are discussed as a potential driver for the low values of R_{GF} in this region.

Figures 5, 7, and S2: Since the authors mentioned about the dependence of HCHO, CHOCHO and RGF on altitude in the main text, I suggest to include the time series of flight altitude in these figures.

As now discussed in section 3.5, R_{GF} is not a function of altitude within the boundary layer. Because the data shown in these figures is primarily or entirely in the boundary layer, altitude plots do not add to this analysis.

Figure 8d: Since the HCHO and CHOCHO measurements shown in a and b are above 200 m, the altitude range should be 200 m – 6 km instead of 0 – 6 km. The zero value of the normalized concentration at 200 m is quite confusing. What is the information the authors want to give by this plot? I could not find it in the main text.

Figure 8d was intended to illustrate the ratio of free troposphere CHOCHO relative to boundary layer CHOCHO is greater than the same ratio for HCHO. As this information can be derived from Figure 8c, and because Figure 8d is a source of confusion, we no longer include Figure 8d in the manuscript.

Figure 9: I suggest to only show the region of the SENEX study, i.e., the region shown in Figure 1.

We prefer to show the whole United States to put the measurements acquired in the SE US in context. Specifically, this map highlights that the SE US, which is dominated by isoprene, and the NW US, which is dominated by monoterpenes, have different values of R_{GF} .

Figures S3 and S4: I suggest to add date and time to each profile number. So that it is clearer to the readers that the change of vertical structure over the time of the day.

The day and time of the profiles are now shown in Figure S4.

References:

Fu, T. M., Jacob, D. J., Wittrock, F., Burrows, J. P., Vrekoussis, M., and Henze, D. K.: Global budgets of atmospheric glyoxal and methylglyoxal, and implications for formation of secondary organic aerosols, *J. Geophys. Res.*, 113, D15303, 10.1029/2007JD009505, 2008.

Lee, Y. N., Zhou, X., Kleinman, L. I., Nunnermacker, L. J., Springston, S. R., Daum, P. H., Newman, L., Keigley, W. G., Holdren, M. W., Spicer, C. W., Young, V., Fu, B., Parrish, D. D., Holloway, J., Williams, J., Roberts, J. M., Ryerson, T. B., and Fehsenfeld, F. C.: Atmospheric chemistry and distribution of formaldehyde and several multioxygenated carbonyl compounds during the 1995 Nashville/Middle Tennessee Ozone Study, *J. Geophys. Res.*, 103, 22449–22462, 10.1029/98jd01251, 1998.

Li, X., Rohrer, F., Brauers, T., Hofzumahaus, A., Lu, K., Shao, M., Zhang, Y. H., and Wahner, A.: Modeling of HCHO and CHOCHO at a semi-rural site in southern China during the PRIDE-PRD2006 campaign, *Atmos. Chem. Phys.*, 14, 12291–12305, 10.5194/acp-14-12291-2014, 2014.

Marais, E. A., Jacob, D. J., Kurosu, T. P., Chance, K., Murphy, J. G., Reeves, C., Mills, G., Casadio, S., Millet, D. B., Barkley, M. P., Paulot, F., and Mao, J.: Isoprene emissions in Africa inferred from OMI observations of formaldehyde columns, *Atmos. Chem. Phys.*, 12, 6219–6235, 10.5194/acp-12-6219-2012, 2012.

Tawfik, A. B., Stöckli, R., Goldstein, A., Pressley, S., and Steiner, A. L.: Quantifying the contribution of environmental factors to isoprene flux interannual variability, *Atmos. Environ.*, 54, 216–224, 10.1016/j.atmosenv.2012.02.018, 2012.

Washenfelder, R. A., Wagner, N. L., Dube, W. P., and Brown, S. S.: Measurement of atmospheric ozone by cavity ring-down spectroscopy, *Environ. Sci. Technol.*, 45, 2938–2944, 10.1021/es103340u, 2011.

Reponse to Interactive comment on “Reassessing the ratio of glyoxal to formaldehyde as an indicator of hydrocarbon precursor speciation” by J. Kaiser et al.

Anonymous Referee #2

We thank the referee for the valuable comments. The original comments are shown in italicized black, while responses are provided below in blue.

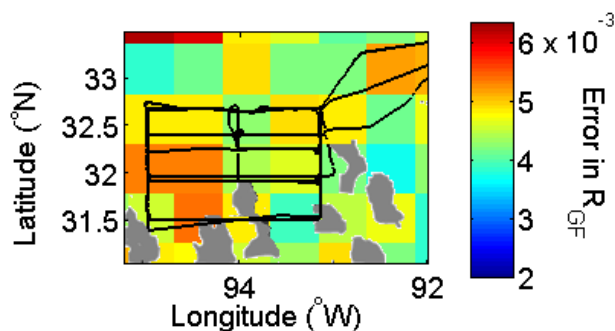
Major comments

1) As pointed out in the paper, the satellite R_{GF} is not well correlated with in situ. The reason given for this discrepancy is the seasonal averaging of the satellite data. When looking more closely, however, some areas such as the Kisatchie forest known to emit monoterpenes, causing high R_{GF} according to SENEX data (as discussed in the manuscript) are not associated to high R_{GF} in satellite data. I believe quite likely that such discrepancy reflects the uncertainties in the measurements, especially from the satellite. The OMI errors deserve more discussion. It is very encouraging to see a better consistency between satellite and in situ R_{GF} data compared to previous studies, but it should be acknowledged that the sources of error for the measurements (especially spaceborne) are plentiful (low signal to noise, interferences from other compounds).

The sources of errors in satellite measurements are numerous, including uncertainties in absorption cross sections, the computation of the air mass factor, instrumental uncertainty (e.g., wavelength calibration), potential interferences from other compounds, and low signal to noise. However, seasonal averaging helps to reduce these errors. Assuming a 15% systematic uncertainty and following the formulation thoroughly explained in Vrekoussis et al. (2010), (section 4.3.1), the average error in satellite R_{GF} over the SE US is 0.005, which is 18% of the average R_{GF} value observed in this region.

This is now discussed in section 2.2.

The error calculated for the pixel over the Kisatchie forest (0.0047) is not larger than errors in other pixels (figure at right: flight track is shown in black, forest in grey). The reviewer is correct that at this scale, pixel-to-pixel variation in R_{GF} is mostly associated with noise. Therefore, the retrievals shown here cannot distinguish the local influence of the forest.



This is now discussed in section 3.5

2) Please cite, and compare your results with the study of Lee et al. (1998) which also provided vertical profiles of formaldehyde, glyoxal and other OVOCs over a BVOC-rich area in the Southeast US. Please provide a plot of the mixing ratios of HCHO and CHOCHO instead of (or in addition to) the profiles given in molec/cm³ (Fig. 8). This would facilitate comparison with previous studies. The Lee et al. study also found slightly higher R_{GF} values in the FT compared to the BL. The possible source for the apparent additional source of glyoxal in the FT is unknown, as pointed out in this manuscript, but it has been hypothesized that the heterogeneous oxidation of aerosols might release glyoxal and other OVOCs, as a possible explanation for high CHOCHO in the FT over the Tropical Pacific (Volkamer et al., 2015). The ozonolysis of fatty acids has indeed been found to be a source of glyoxal and other compounds (Zhou et al., 2014).

We now include a quantitative comparison of our measurements and the Lee et al. (1998) measurements in section 3. Figure 8 has been remade to show HCHO and CHOCHO in units of ppb. Comparison with R_{GF} vertical profiles observed by Lee et al. (1998) and Li et al. (2014) is now included in section 3.5. Section 3.5 also now mentions the possibility of heterogeneous oxidation of aerosols as a CHOCHO source in the F.T.

Minor comments

2.2, p. 6244: Provide some discussion of the uncertainties in the satellite retrievals

See response to major comment #1.

p. 6246, line 2: which monoterpenes are emitted by longleaf pines? Frankin and Snyder (1971) mention alpha-pinene and 1-pinene, but there should be more recent studies. This is relevant as there might possibly be large differences between the glyoxal yields of different monoterpenes.

We now cite a more recent study which details the relative emissions rates of speciated monoterpenes from longleaf pines (*Pinus palustris*). The emission rate of β-pinene is the largest, approximately 30% greater than the α-pinene emission rate. All other monoterpene emissions are at least an order of magnitude lower (Geron et al., 2000). The modeled relative abundance of HCHO and CHOCHO from the oxidation of α-pinene and β-pinene is included in Table 2.

p. 6248, l. 6: "Isoprene is still likely the dominant OVOC precursor": true, but aren't there means to prove that hypothesis?

Proving this requires modeling the complete HCHO and CHOCHO budgets, which is beyond the scope of this work. However, we now state that isoprene is a much larger source of OH reactivity than anthropogenic VOCs. This strongly supports our conclusion that isoprene is likely the largest source of both HCHO and CHOCHO.

p. 6248, l. 14-16: Yes, ISOP_{OOH} can interfere with MVK+MACR measurement, but this does not weaken the argument that oxidation occurs faster in the plume, since ISOP_{OOH} is also isoprene oxidation product.

If ISOPOOH creates a positive bias MVK+MACR measurement, the artifact would be larger in the low-NO_x areas, artificially increasing the (MVK+MACR)/isoprene ratio observed outside of the plume. Because (MVK+MACR)/isoprene is higher inside the plume, any interference would not affect the conclusion that oxidation occurs faster in the plume. This is now stated in the manuscript.

p. 6249-6250 (Section 3.4) and Table 2: Are the AVOCs of Table 2 the only significant contributions to CHOCHO (not mentioning CH₂O)? What about C₂H₄, C₂H₂, ...?

While ethene and ethyne are not expected to contribute significantly to the HCHO and CHOCHO budgets, they are now included in Table 2 and discussed in section 3.4. By providing results for increasing length of alkane (ethane to butane) and also bond order (ethane to ethyne), we provide one example of the effect of precursor structure on resultant R_{GF}.

Minor/technical remarks

p. 6245, l. 26 'On both the 10 June and 25th flights' is awkward, please rephrase.

p. 6248, l. 21: insert "are" after "in-plume"

p. 6249, l. 5: insert "%" after (2.2 ± 0.2)

p. 6249, l. 14-16: Low-NO_x isoprene oxidation is not well understood also (a fortiori) for glyoxal formation, not just CH₂O and OH.

p. 6252, l. 13-16: the sentence "In general, profiles... is less" is awkward. You could e.g. remove the two last words.

p. 6253, l. 13: the year should be 2014 for Gonzalez Abad.

p. 6254, l. 18: please insert "broadly" before "in agreement for the two platforms" given the reservations outlined above.

We thank the reviewer for the careful reading. All minor/technical remarks have been addressed.

References:

Geron, C., Rasmussen, R., Arnts, R. R., and Guenther, A.: A review and synthesis of monoterpene speciation from forests in the United States, *Atmos. Environ.*, 34, 1761-1781, 10.5194/acp-5-1053-2005, 2000.

Lee, Y. N., Zhou, X., Kleinman, L. I., Nunnermacker, L. J., Springston, S. R., Daum, P. H., Newman, L., Keigley, W. G., Holdren, M. W., Spicer, C. W., Young, V., Fu, B., Parrish, D. D., Holloway, J., Williams, J., Roberts, J. M., Ryerson, T. B., and Fehsenfeld, F. C.: Atmospheric chemistry and distribution of formaldehyde and several multioxygenated carbonyl compounds during the 1995 Nashville/Middle Tennessee Ozone Study, *J. Geophys. Res.*, 103, 22449–22462, 10.1029/98jd01251, 1998.

Li, X., Rohrer, F., Brauers, T., Hofzumahaus, A., Lu, K., Shao, M., Zhang, Y. H., and Wahner, A.: Modeling of HCHO and CHOCHO at a semi-rural site in southern China

during the PRIDE-PRD2006 campaign, *Atmos. Chem. Phys.*, 14, 12291-12305,
10.5194/acp-14-12291-2014, 2014.

1 **Reassessing the ratio of glyoxal to formaldehyde as an**
2 **indicator of hydrocarbon precursor speciation**

3
4 **J. Kaiser¹, G. M. Wolfe^{2,3}, K. E. Min^{4,5,*}, S. S. Brown^{5,6}, C. C. Miller⁷, D. J. Jacob^{7,8}, J.**
5 **A. deGouw^{4,5}, M. Graus^{4,5}, T. F. Hanisco³, J. Holloway^{4,5}, J. Peischl^{4,5}, I. B.**
6 **Pollack^{4,5}, T. B. Ryerson⁵, C. Warneke^{4,5}, R. A. Washenfelder^{4,5}, and F. N.**
7 **Keutsch^{1,**}**

8
9 ¹Department of Chemistry, University of Wisconsin-Madison, Madison, WI, USA

10 ²Joint Center for Earth Systems Technology, University of Maryland Baltimore County,
11 Baltimore, Maryland, USA

12 ³Atmospheric Chemistry and Dynamics Laboratory, NASA Goddard Space Flight Center,
13 Greenbelt, Maryland, USA

14 ⁴Cooperative Institute for Research in Environmental Sciences, University of Colorado Boulder,
15 Boulder, Colorado, USA

16 ⁵Chemical Sciences Division, NOAA Earth System Research Laboratory, Boulder, Colorado,
17 USA

18 ⁶Department of Chemistry and Biochemistry, University of Colorado, Boulder, Colorado, USA

19 ⁷Department of Earth and Planetary Sciences, Harvard University, Cambridge, Massachusetts,
20 USA

21 ⁸School of Engineering and Applied Sciences, Harvard University, Cambridge, Massachusetts,
22 USA

23 ^{*}now at School of Environmental Science and Engineering, Gwangju Institute for Science and
24 Technology, Gwangju, Korea

Formatted: Font color: Auto

Formatted: Font color: Auto

Formatted: Font color: Auto

Formatted: Font color: Auto, English (United States)

Formatted: Font color: Auto

1 | **now at School of Engineering and Applied Sciences and Department of Chemistry and
2 | Chemical Biology, Harvard University, Cambridge, Massachusetts, USA
3 | Correspondence to: [J. Kaiser \(jen.b.kaiser@gmail.com\)](mailto:jen.b.kaiser@gmail.com)

Formatted: Font color: Auto

Abstract

The yield of formaldehyde (HCHO) and glyoxal (CHOCHO) from oxidation of volatile organic compounds (VOCs) depends on precursor VOC structure and the concentration of ~~NO_x~~ ~~(NO_xNO_x (NO_x = NO + NO₂))~~. Previous work has proposed that the ratio of CHOCHO to HCHO (R_{GF}) can be used as an indicator of precursor VOC speciation, and absolute concentrations of the ~~oxidation products~~ CHOCHO and HCHO as indicators of ~~NO_xNO_x~~. Because this metric is measurable by satellite, it is potentially useful on a global scale; however, absolute values and trends in R_{GF} have differed between satellite and ground-based observations. To investigate potential causes of previous discrepancies and the usefulness of this ratio, we present measurements of CHOCHO and HCHO over the Southeast United States (SE US) from the 2013 SENEX flight campaign, and compare these measurements with OMI satellite retrievals. High time-resolution flight measurements show that high R_{GF} is associated with monoterpene emissions, low R_{GF} is associated with isoprene oxidation, and emissions associated with oil and gas production can lead to small-scale variation in regional R_{GF} . During the summertime in the SE US, R_{GF} is not a reliable diagnostic of anthropogenic VOC emissions, as HCHO and CHOCHO production are dominated by isoprene oxidation. Our results show that the new glyoxal CHOCHO retrieval algorithm reduces the previous disagreement between satellite and in situ R_{GF} observations. WeAs the absolute values and trends in R_{GF} observed during SENEX are largely reproduced by OMI observations, we conclude that satellite-based observations of R_{GF} can be used alongside other measurements knowledge of land-use as a global diagnostic of ~~the chemical conditions leading to secondary pollutant formation~~ dominant hydrocarbon speciation.

Formatted: Font color: Auto

1 Introduction

Though volatile organic compounds (VOCs) are present only in trace amounts in the atmosphere, their presence can drive the formation of pollutants such as secondary organic aerosol and ozone. The impact of VOC emissions on tropospheric chemistry depends on the speciation of emitted VOCs and their degradation pathways. As many as 10^5 different species of VOCs are estimated to have been measured in the atmosphere (Goldstein and Galbally, 2007). While an air mass will

1 usually contain a large variety of VOCs, often a particular species or subset of species (e.g.
2 biogenics) will dominate the photochemistry, giving rise to the production of a range of
3 oxygenated VOCs (OVOCs). Thus, OVOCs can provide downstream constraints on the rates and
4 pathways of VOC oxidation.

5 Here, we focus on the production of two ubiquitous OVOCs: formaldehyde (HCHO) and glyoxal
6 (CHOCHO). HCHO is formed from the oxidation of nearly every anthropogenic and biogenic
7 VOC (AVOC/BVOC, respectively). Though photochemical formation is thought to dominate the
8 HCHO global budget (Fortems-Cheiney et al., 2012), direct HCHO emissions from pyrogenic,
9 anthropogenic, and biogenic activity have also been observed (Guenther et al., 1995;
10 Kesselmeier et al., 1997; Holzinger et al., 1999; Garcia et al., 2006; DiGangi et al., 2011).
11 CHOCHO is formed from the oxidation of a smaller subset of VOCs, particularly alkenes,
12 ~~aromatics, isoprene, and aromatic compounds~~ ~~monoterpenes~~, (Fu et al., 2008). Direct emission
13 from biofuel and biomass burning can also be a significant source of CHOCHO (McDonald et
14 al., 2000; Hays et al., 2002; Christian et al., 2003; Greenberg et al., 2006). Because the
15 ~~yield/yields~~ of HCHO and CHOCHO ~~differs/differ~~, between classes of VOC, and because their
16 atmospheric lifetimes are similar, the relative abundance of CHOCHO and HCHO has been
17 hypothesized to reflect the speciation of VOCs contributing to total VOC reactivity (Vrekousiss
18 et al., 2010; DiGangi et al., 2012; MacDonald et al., 2012; Li et al., 2014; Miller et al., 2014).

19 A major motivating factor for examining the ratio of glyoxal to formaldehyde (R_{GF} , in units of
20 mole/mole) is the ability to quantify both compounds on a global scale from satellite retrievals.
21 Currently, HCHO and CHOCHO are the only two OVOCs with UV-Visible absorption features
22 strong enough to enable solar backscatter measurements of vertical column ~~density~~
23 ~~(~~ved~~)-densities~~. Long term continuous HCHO columns are available from four satellite-based
24 instruments: GOME (Global Ozone Monitoring Experiment), SCIAMACHY (Scanning Imaging
25 Absorption spectroMeter for Atmospheric CHartographY), OMI (Ozone Monitoring Instrument),
26 and GOME-2. CHOCHO retrievals are available from SCIAMACHY, OMI, and GOME-2.
27 Satellite-derived R_{GF} could be a promising diagnostic tool in determining the speciation of VOC
28 precursors that lead to pollution formation in a given region, especially as retrievals improve in
29 temporal and spatial resolution.

Formatted: Font color: Auto

1 Table 1 summarizes previously published observations and conclusions about R_{GF} . Using
2 GOME-2 satellite retrievals, Vrekoussis et al. (2010) observed R_{GF} as low as 3% in
3 anthropogenic regions and between 4 and 6% over heavily vegetated regions. This was
4 interpreted as an indication that anthropogenic precursors favor HCHO production relative to
5 CHOCHO, while biogenic precursors favor CHOCHO production relative to HCHO. Primary
6 emissions of HCHO were also thought to lower the observed R_{GF} in anthropogenic regions. In
7 contrast, using ground-based measurements, DiGangi et al. (2012) observed R_{GF} values typically
8 $< 2\%$ in rural areas, while fresh anthropogenic influence increased R_{GF} to 4%. These observations
9 yielded a directly contradictory interpretation: AVOCs favor CHOCHO production, whereas
10 BVOCs favor HCHO production. Furthermore, DiGangi et al. (2012) showed that, given the
11 same VOC speciation, R_{GF} was invariant despite changes in observed NO_x/NO_x concentrations.
12 They proposed that this was a result of CHOCHO and HCHO formation primarily via the high-
13 NO_x/NO_x pathway of organic peroxy radical (RO_2) reactions, which in turn makes the absolute
14 concentration of either OVOC equally dependant on NO_x/NO_x and therefore leaves R_{GF}
15 unchanged.

16 Following these two investigations, high values of R_{GF} (20-40%) were observed above an Asian
17 tropical forest (MacDonald et al., 2012), agreeing qualitatively with the conclusion of Vrekoussis
18 et al. that high R_{GF} is consistent with biogenic source areas. The reported R_{GF} values, however,
19 are an order of magnitude greater than satellite observations (Vrekoussis et al., 2010; Miller et
20 al., 2014). Li et al. (2014) report an average R_{GF} of 6% at a semi-rural site in Southern China.
21 Both observations and model simulations showed that increasing AVOC emissions lead to an
22 increase in R_{GF} . The model simulations indicated R_{GF} was controlled not only by VOC
23 speciation, but also by ~~the~~ NO_x/NO_x and OH mixing ratios, as well as physical processes such as
24 CHOCHO deposition and aerosol uptake (Li et al., 2014). Recently, a new algorithm for the
25 retrieval of ~~glyoxal~~ CHOCHO from OMI was developed which lessens sensitivity to water vapor
26 abundance and produces on-average lower CHOCHO ~~vertical column densities~~, due to the
27 choice of reference sector (Miller et al., 2014). In contrast to the ranges of R_{GF} reported by
28 Vrekoussis et al. (2010), the OMI retrieval yields high R_{GF} in areas associated with monoterpene
29 emissions, intermediate R_{GF} in areas dominated by anthropogenic emissions, and low R_{GF} in
30 regions associated with strong isoprene emissions.

Formatted: Font color: Auto

1 The cause of the discrepancies between satellite and ground-based R_{GF} trends and absolute
2 values are unknown. DiGangi et al. (2012) suggested column-integrated and ground-based
3 measurements in forests may differ due to direct HCHO emissions, or boundary layer ratios
4 could be systematically lower than free troposphere ratios. Additionally, Miller et al. (2014)
5 highlight interferences from water vapor, reference sector selection, and multi-year averaging as
6 potential causes for the previous errors in satellite retrievals. Despite the different ranges and
7 trends of observed values, all previously published work concludes that R_{GF} reflects at least in
8 part the speciation of VOCs in a given air mass. If R_{GF} is to be used as a global tracer of VOC
9 composition, all factors influencing R_{GF} must be fully elucidated, and satellite retrievals must be
10 validated against field observations.

11 With flights transecting both anthropogenic and biogenic regions, as well as profiles **extending**
12 from the boundary layer into the free troposphere, the 2013 SENEX (Southeast Nexus) field
13 campaign provides an unprecedented opportunity to address these uncertainties. Unlike ground-
14 based field campaigns, the flight campaign provides information about the vertical structure of
15 the trace gasses and a direct, real-time comparison of R_{GF} in urban outflow and in the
16 surrounding rural areas. To our knowledge, this data represents the first high-time resolution
17 simultaneous in situ flight-based measurements of HCHO and CHOCHO. We present absolute
18 mixing ratios of HCHO and CHOCHO observed during daytime flights in the Southeast United
19 States (SE US) and discuss the observed relationships of R_{GF} with observed VOC precursors and
20 anthropogenic influence. Finally, to investigate the applicability of our findings for global
21 studies, we compare flight-based R_{GF} with those derived from OMI observations.

23 **2 Experimental Methods**

24 **2.1 SENEX flight measurements**

25 During the SENEX project in June and July of 2013, HCHO, CHOCHO, ~~NO_xNO_x~~, and VOC
26 measurements were acquired simultaneously from the NOAA WP-3D research aircraft during 13
27 daytime flights. An in-depth description of the SENEX science goals, NOAA WP-3D aircraft, all
28 onboard instrumentation, and each flight plan can be found elsewhere (C. Warneke, in

Formatted: Font color: Auto

Formatted: Font color: Auto

1 preparation, 2014, 2015). A summary of average conditions for each flight is provided in Table
2 S1.

Formatted: Font color: Auto

3 HCHO was measured at 1 Hz by the NASA In Situ Atmospheric Formaldehyde (ISAF)
4 instrument (Cazorla et al., 2014), which is based on the Fiber-Laser-Induced-Fluorescence
5 (FILIF) technique (Hottle et al., 2009; DiGangi et al., 2011; Kaiser et al., 2014). The reported
6 accuracy of the HCHO measurements is 10%. CHOCHO was measured at 0.2 Hz by Airborne
7 Cavity Enhanced Spectrometer (ACES) with 6% accuracy. (Washenfelder et al., 2011; K. Min,
8 in preparation, 2014, 2015). The precision of the CHOCHO measurement was a significant
9 fraction of the typical ambient concentration (32 ppt precision, with a typical concentration of
10 100-150 pptv), such that precision is a more stringent limitation on data quality than accuracy
11 relative to HCHO, for which the signal was consistently much larger (HCHO precision 25 ppt,
12 with concentrations typically > 3 ppb).

Formatted: Font color: Auto

13 NO and NO₂ were measured by ozone-induced chemiluminescence (CL) and UV photolysis
14 followed by CL, respectively (Ryerson et al., 1998; Pollack et al., 2012). VOCs were measured
15 at 20% accuracy using proton-transfer reaction mass spectrometry (de Gouw and Warneke,
16 2007). Unless otherwise specified, all data shown here are filtered to remove in-cloud
17 measurements, measurements below 200 m or above 1200 m, and data that may be affected by
18 the exhaust of the WP-3D aircraft. R_{GF} is calculated by averaging the 1 s HCHO data to the 5 s
19 CHOCHO observations.

20 2.2 Satellite retrievals

21 The Ozone Monitoring Instrument (OMI) is a nadir viewing UV-Visible grating spectrometer,
22 launched onboard the NASA Aura satellite in July 2004 (Levelt et al., 2006). OMI provides daily
23 global coverage at high spatial resolution (13 x 24 km footprint at nadir). We use slant
24 ~~columns~~ ~~(Ω_s)~~ column densities (Ω_s) of HCHO and CHOCHO from 2006 to 2007 derived from fits to OMI
25 spectra (González Abad et al., 2014; Miller et al., 2014). HCHO and CHOCHO are retrieved
26 between 328.5-365.5 nm and 435-461 nm respectively. Slant columns are adjusted to vertical
27 ~~columns~~ ~~(Ω_v)~~ column densities (Ω_v) using scattering weights (~~$S(z)$~~) archived from the

Formatted: Font color: Auto, Lowered by 6 pt

Formatted: Font color: Auto

Formatted: Font color: Auto, Lowered by 6 pt

Formatted: Font color: Auto

Formatted: Font color: Auto, Lowered by 5 pt

Formatted: Font color: Auto

1 retrieval product, and species concentration profiles (~~$n(z)$~~ $n(z)$) from the GEOS-Chem chemical
2 transport model (v9-01-03) (Bey et al., 2001; Mao et al., 2013).

$$3 \quad \Omega_v = \Omega_s \frac{\int_0^\infty n(z) dz}{\int_0^\infty S(z)n(z) dz} \quad \Omega_v = \Omega_s \frac{\int_0^\infty n(z) dz}{\int_0^\infty S(z)n(z) dz} \quad (1)$$

4 Here we use daily GEOS-Chem profiles spanning the observation period averaged between
5 13:00-14:00 local time (LT), close to the satellite equatorial crossing time (13:38 LT). The
6 satellite observations are gridded as ~~multi-year~~ seasonal averages on a 0.5° x 0.5° (lat x lon) grid.

7 In this analysis, we use the averaged vertical column densities for June through August of 2007.

8 The overlap between the satellite footprint and output grid is accounted for using an area-
9 weighted tessellation algorithm (Liu et al., 2006). Satellite pixels with cloud fractions larger than
10 0.2 (derived from the OMI O₂-O₂ cloud algorithm (Stammes et al., 2008) and those impacted by
11 the row anomaly (<http://www.knmi.nl/omi/research/product/rowanomaly-background.php>) are
12 filtered before gridding.

13 The sources of errors in satellite measurements are numerous, including uncertainties in
14 temperature-dependent absorption cross sections, the computation of the air mass factor,
15 instrumental errors (e.g., wavelength calibration), potential interferences from other compounds,
16 and low signal to noise. Seasonal averaging helps to reduce these errors. Assuming a 15%
17 systematic uncertainty and following the formulation thoroughly explained in Vrekoussis et al.
18 (2010), (section 4.3.1), the average error in satellite R_{GF} over the SE US is 0.005, which is 18%
19 of the average R_{GF} value observed in this region.

21 3 Results and Discussion

22 Figure 1 shows ~~daytime~~ daytime SENEX flight tracks colored by HCHO, CHOCHO, and R_{GF}, with major
23 emissions sources also indicated. Emissions information was acquired from the Continuous
24 Emissions Monitoring Systems dataset for July - September of 2012
25 (<http://ampd.epa.gov/ampd/>). In general, ~~CHOCHO and CHOCHO~~ HCHO and CHOCHO mixing ratios are higher
26 in the areas associated with high BVOC emissions (southern flights). In particular, high HCHO

Formatted: Font color: Auto, Lowered by 5 pt

Formatted: Font color: Auto

Formatted: Font color: Auto, English (United States)

Formatted: Font color: Auto

Formatted: Font color: Auto, English (United States)

Formatted: Font color: Auto

Formatted: Font color: Auto

1 is observed over the Ozarks “isoprene volcano” (Wiedinmyer et al., 2005). ~~Both~~The
2 concentrations of both OVOCs are ~~enhanced over their background level~~higher, in regions with
3 anthropogenic influence ~~than in the surrounding biogenically dominated areas~~. Compared to the
4 northern cities of Indianapolis and St. Louis, Birmingham and Atlanta have higher mixing ratios
5 of HCHO and CHOCHO in their outflows. The Haynesville shale region has higher mixing
6 ratios of both OVOCs, and CHOCHO is especially enhanced. While HCHO and CHOCHO
7 mixing ratios each vary by more than a factor of 4, the overall variability of R_{GF} observed during
8 the SENEX flight campaign is low.

9 Boundary HCHO and CHOCHO measurements were also acquired during the Nashville/Middle
10 Tennessee Ozone Study in June/July of 1995. While SENEX flight tracks more heavily sampled
11 oil and natural gas fields, both studies are mainly representative of the isoprene-rich SE US. The
12 average HCHO mixing ratio is similar (4.2 ppb in 1995, 4.4 ppb in this study), as is the average
13 CHOCHO mixing ratio (0.07 ppb in 1995, 0.10 ppb in this study), leading to similar R_{GF} (1.7%
14 in 1995, and 2.2% in this study) (Lee et al., 1998).

15 Figure 2 shows the same SENEX flight data gridded to the resolution of the OMI satellite
16 retrievals ($0.5^\circ \times 0.5^\circ$). Removing the flights with distinctly high or low R_{GF} observations (June
17 10th, June 25th, and June 26th) the average gridded R_{GF} is $2.5\% \pm 0.5\%$, with a correlation
18 coefficient between HCHO and CHOCHO of $r^2 = 0.70$. Below, we discuss these regions of
19 notably high and low R_{GF} as well as the influence of urban emissions on the ratio.

20 Variability in the time of measurement may have an impact on the comparison of absolute
21 concentrations of ~~both~~ OVOCs and R_{GF} , as measurements were acquired over a range of mid-day
22 hours (~10:00-17:00 local time, see Table S1), and both HCHO and CHOCHO have strong
23 diurnal cycles. By comparing ~~measurements acquired~~the observations made within 1 hour, on a
24 single given flight over a short time scale, ~~the same day~~, we aim to minimize any impact diurnal
25 variation of R_{GF} would have on this analysis.

26 3.1 Regions of high R_{GF}

27 On both the~~During flights on 10 June 10th and 25th flights~~25 June, the region responsible for the
28 high observed R_{GF} (4-7%) is in the southeast corner of the flight track, over the Kisatchie

Formatted: Font color: Auto

1 National Forest (Fig. 3a, 3b). The dominant tree species in this region is longleaf pine
2 (<http://www.wlf.louisiana.gov>), ~~reported to emit monoterpenes (Rasmussen, 1972).~~
3 ~~Monoterpene~~. Longleaf pine (*Pinus palustris*) is reported to emit monoterpenes but not isoprene
4 (Rasmussen, 1972). ~~The measured emission rate of β -pinene is the largest, and approximately~~
5 ~~30% greater than the α -pinene emission rate. All other monoterpenes emission rates are at least~~
6 ~~an order of magnitude lower (Geron et al., 2000). Indeed, measured monoterpene~~ mixing ratios
7 are elevated over this portion of the flight track (Fig. 3c, 3d), while isoprene (not shown) is
8 relatively constant over the footprints of both flights. The high-monoterpene/high- R_{GF}
9 relationship is in agreement with the Miller et al. (2014) satellite observation of high R_{GF} values
10 above the boreal forests, where the high CHOCHO yield of monoterpenes is cited as the primary
11 driver of R_{GF} (Fu et al., 2008). As in the two flights over the Kisatchie Forest, the June 26th flight
12 also highlights a region with high monoterpenes and $R_{GF} > 3\%$ (arrow on Fig. 4).

Formatted: Font color: Auto

13 Also on the June 25th flight, high R_{GF} ($>8\%$) is seen on the northeast side of the flight track
14 (circled on Fig. 3b and 3d). Unlike the high R_{GF} associated with the monoterpenes emissions,
15 these values are not replicated in the same area during the June 10th flight. In this region, R_{GF} is
16 driven by a decrease in HCHO mixing ratio while the CHOCHO mixing ratio is slightly elevated
17 (Fig. 5). Sharp features in meteorological measurements such as potential temperature, an
18 increase in ozone, and a decrease in all other VOC and OVOC mixing ratios suggest an incursion
19 of free tropospheric air. Given the lack of VOC precursors and other oxidation products, and
20 assuming it is not a measurement artifact, the source of CHOCHO in the free troposphere is still
21 unknown. The effect of trace gas vertical profile structure on the analysis of R_{GF} is examined in
22 further detail in section 3.4.

23 3.2 Regions of low R_{GF}

24 On the June 26th flight ~~upwind, north~~ of the gas production near the eastern side of the flight
25 track, CHOCHO concentrations are low while HCHO mixing ratios are typical of other SENEX
26 observations, driving R_{GF} to near 0% (Fig. 4). Concentrations of BVOC and AVOC precursors
27 are also low in this region; however, methane ~~and CO_2~~ mixing ratios are dramatically elevated.
28 ~~increased~~ While isoprene is the dominant VOC in terms of calculated OH reactivity, ~~increased~~
29 HCHO relative to CHOCHO could be a result of oxidation of alkanes, which are associated with

Formatted: Font color: Auto

Formatted: Font color: Auto

Formatted: Font color: Auto

1 oil and natural gas (O&NG) production (Gilman et al., 2013). Gas flaring could also be a large
2 source of direct HCHO emissions (Pikelnaya et al., 2013).

3 On the portion of the June 26th flight flown over the Mark Twain National Forest in ~~eastern the~~
4 Missouri ~~Ozarks~~ (Fig. 4), the average R_{GF} is $1.1 \pm 0.2\%$. Here, the average isoprene
5 concentration is high (7 ± 2 ppb), ~~NO_xNO_x~~ is low (0.23 ± 0.02 ppb), and AVOC concentrations
6 are low compared to BVOCs (toluene = 0.06 ± 0.01 ppb). This suggests relatively pristine
7 regions with strong isoprene emissions can be characterized by low R_{GF} . It is important to note
8 that these measurements were acquired later in the day than most other measurements (~2:30
9 L.T. Table S1), and approximately 3 hours later than the measurements acquired on the
10 southwest portion of the flight track. We thus cannot rule out diurnal variation as an influence on
11 R_{GF} in this region.

12 3.3 Urban influence on R_{GF}

13 ~~As shown in Table 1, NO_x and~~ Because R_{GF} may be influenced by AVOC emissions ~~have been~~
14 ~~proposed to influence R_{GF} in multiple ways, and therefore R_{GF} and/or NO_x (Table 1), it~~ has been
15 ~~proposed that R_{GF} can be used~~ a diagnostic of the chemistry that leads to O₃ formation ~~in urban~~
16 ~~areas~~ (Vrekousiss et al., 2010; DiGangi et al., 2012; Li et al., 2014). Potential explanations for
17 varying R_{GF} in urban areas include (1) preferential formation of one OVOC from AVOCs, (2)
18 ~~differing NO_x dependencies of OVOC yields, and (3) faster oxidation caused by high OH leading~~
19 ~~to different relative concentrations of the OVOCs, and (3) differing NO_x dependencies of~~
20 OVOC yields.

21 A comparison of in-plume and surrounding background measurements from the June 12th flight
22 through Atlanta can help determine which of these factors may contribute to differences in
23 observed R_{GF} . During this flight, northwesterly winds brought emissions from a nearby paper
24 mill and power plant over the Atlanta area. As it travelled, the plume encountered emissions
25 from the Atlanta international airport and other point and area sources. Figure 6 shows the flight
26 path colored by CO, which demonstrates the boundary between background and polluted air.
27 Figure 7 shows the mixing ratios of isoprene, toluene, ~~NO_xNO_x~~, HCHO, CHOCHO, and
28 OVOCs, as well as the observed R_{GF} for the first four transects downwind of Atlanta.

Formatted: Font color: Auto

1 Inside the plume, ~~NO_xNO_x~~ is enhanced, AVOCs such as toluene are high, BVOC mixing ratios
2 are low, and concentrations of both OVOCs increased significantly (Fig 7). However, no clear
3 distinction between in-plume and background measurements can be seen in R_{GF}. This trend in
4 increasing HCHO and CHOCHO but consistent R_{GF} is also seen in several other flight tracks
5 following urban outflow (for further examples, see Fig. S1 and S2 highlighting the July 5th flight
6 over St. Louis).

Formatted: Font color: Auto

7 There are two potentially compounding causes of the increase in ~~OVOCs~~, HCHO and CHOCHO
8 concentrations. First, direct emissions of the OVOCs or oxidation of AVOCs in the plume add to
9 the background concentrations of HCHO and CHOCHO. While the oxidation of the observed
10 AVOCs will increase OVOCs, the contribution of isoprene and its first generation oxidation
11 products methyl-vinyl-ketone (MVK) and methacrolein (MACR) to OH reactivity is more than a
12 factor of 10 times greater than the contribution from measured AVOCs. Therefore, isoprene is
13 still likely the dominant ~~OVOC~~HCHO and CHOCHO precursor. Second, higher ~~NO_xNO_x~~ in the
14 plume leads to more efficient oxidation of VOCs, depleting mixing ratios of primary VOCs such
15 as isoprene and increasing its oxidation products. This is consistent with the classical ~~NO_xNO_x~~-
16 dependence of OH concentrations (Rohrer et al., 2014). The ratio of the first generation isoprene
17 oxidation products methyl vinyl ketone (MVK) and methacrolein (MACR) to isoprene can be
18 used as an indicator of the extent of photochemical processing (Fig. 7). The higher in-plume ratio
19 of MVK+MACR to isoprene supports the conclusion that oxidation occurs faster in the plume,
20 though it. It is important to note that the low-~~NO_xNO_x~~ oxidation product ISOPOOH (isoprene
21 hydroxy hydroperoxide) can interfere with PTR-MS measurements of MVK+MACR (Rivera-
22 Rios et al., 2014), and potentially also measurements of HCHO.- If ISOPOOH creates a positive
23 bias MVK+MACR measurement, the artifact would be larger in the low-NO_x areas, artificially
24 increasing the (MVK+MACR)/isoprene ratio observed outside of the plume. Because
25 (MVK+MACR)/isoprene is higher inside the plume, any interference would not affect the
26 conclusion that oxidation occurs faster in the plume.

Formatted: Font color: Auto

Formatted: Font: Italic, Font color: Auto

27 The absolute concentrations of ~~OVOCs~~HCHO and CHOCHO point to more rapid oxidation of
28 isoprene in-plume as well as a potentially small contribution of AVOCs to ~~the both~~ overall
29 OVOC ~~budget~~budgets, but neither of these characteristics influence R_{GF}. As stated above, a third
30 potential driver of R_{GF} is a difference in high- and low-~~NO_xNO_x~~ oxidation mechanisms. Again,

Formatted: Font color: Auto

1 though the ~~NO_xNO_x~~ concentrations observed in-plume ~~are~~ significantly different than the
2 surrounding air such that RO₂ spans different fates (reaction with NO versus reaction with HO₂
3 and isomerization), no characteristic change in R_{GF} is observed. Therefore, R_{GF} cannot be used to
4 diagnose AVOC emissions, RO₂ fate, or OH levels in urban areas where isoprene emissions
5 dominate the ~~OVOC budget~~~~HCHO and CHOCHO budgets~~.

Formatted: Font color: Auto

Formatted: Font color: Auto

6 As discussed in section 3.2, the Ozarks demonstrated especially low R_{GF}. Both the Atlanta
7 background air and the Ozarks are low-~~NO_xNO_x~~ isoprene-dominated regions (0.5 ppb ~~NO_xNO_x~~
8 near Atlanta, 0.2 ppb ~~NO_xNO_x~~ in the Ozarks), yet R_{GF} observations in these areas are
9 significantly different. As previously discussed, urban emissions do not cause significant
10 changes in R_{GF} if isoprene is the dominant VOC; therefore, some other factor must contribute to
11 the comparably low R_{GF} over the Ozarks. While the observations of R_{GF} over the Ozarks were
12 acquired at ~14:20 L.T., later observations of R_{GF} in the plume background are not significantly
13 different than the earlier observations shown in Figure 7 (R_{GF} of ~~2.2 ± ± 0.3%~~ between 14:00 and
14 14:30 L.T.~~→~~~~→~~). This suggests that diurnal variation of R_{GF} is not the driving cause of the difference
15 between Atlanta and Ozark observations.

Formatted: Font color: Auto

16 The most notable difference between the regions is the observed concentrations of isoprene.
17 Isoprene reached over 10 ppb in the Ozarks, while the Atlanta background air reached only 4
18 ppb. A stronger relative contribution of monoterpenes to the ~~OVOC budget~~~~HCHO and~~
19 ~~CHOCHO budgets~~ in Atlanta could result in the higher observed R_{GF} (~50 ppt monoterpene/ppb
20 isoprene near Atlanta, ~15 ppt monoterpenes/ppb isoprene near the Ozarks). Alternatively, the
21 relationship of HCHO and CHOCHO with isoprene may be non-linear, with higher isoprene
22 emissions leading to lower R_{GF}. Because low-~~NO_xNO_x~~ isoprene oxidation is not well
23 understood, especially with respect to OH concentrations (Rohrer et al., 2014)~~→~~~~→~~ and~~→~~ HCHO
24 yields (Palmer et al., 2006; Marais et al., 2012)~~→~~ and CHOCHO yields (Stavrakou et al., 2009),
25 model analysis cannot conclusively determine the cause of decreasing R_{GF} with increasing
26 isoprene emissions. A model can be useful, however, in determining the anticipated influence of
27 hydrocarbon speciation on R_{GF}, as discussed below.

Formatted: Font color: Auto

Formatted: Font color: Auto

Formatted: Font color: Auto

Formatted: Font color: Auto

3.4 Modeled trends in R_{GF} with hydrocarbon speciation

The values of R_{GF} presented above suggest that (1) monoterpene oxidation leads to higher R_{GF} than isoprene, (2) AVOCs must have substantially high concentrations to affect R_{GF} in regions with high isoprene emissions, and (3) depending on the surrounding BVOC emissions, alkanes could decrease the regional R_{GF} . To examine if these results are consistent with our understanding of the oxidation mechanisms of each VOC precursor, a simple 0-D box model analysis was performed using the University of Washington Chemical Box Model (UWCM) (Wolfe and Thornton, 2011), which incorporates the Master Chemical Mechanism v 3.2 (Jenkin et al., 1997; Saunders et al., 2003).

The intent of these model scenarios is not to compare modeled concentrations of CHOCHO and HCHO to their observed values, nor to compare modeled and measured R_{GF} , but to investigate the relative values of R_{GF} predicted by the model for each VOC precursor. Temperature, relative humidity, O_3 , and CO are held at their observed campaign averages (297 K, 70%, 51 ppb, and 140 ppb, respectively). OH is held at 4×10^6 molec/cm³, and NO_x is constrained to the measured values representative of the plume background on 12 June 12th (NO = 0.06 ppb; NO₂ = 0.41 ppb). The solar zenith angle is set to 13.4°, representative of the sun's position over Atlanta at 12:00 local time on June 12th. Pressure is set to a constant 760 Torr, and all species are given an additional sink with a lifetime of 24 hours in lieu of explicitly modeling physical loss processes like deposition and dilution. The only hydrocarbon present in each model scenario is the VOC of interest, held at a constant concentration of 1 ppb. Integration time is set to 5 days, at which point the concentrations of both OVOCs are nearly constant. The calculated mixing ratios of CHOCHO and HCHO at the end of the model runs are shown in Table 2.

Compared to isoprene, the two monoterpenes investigated here (α - and β -pinene) produce more CHOCHO per HCHO. As this effect has been demonstrated in model calculations, satellite observations, and flight-based measurements, we conclude that observations of high values of R_{GF} are a result of high monoterpene compared to isoprene emissions. The absolute concentrations of both OVOCs produced from the oxidation of AVOCs studied here (benzene, toluene, ethene, ethyne, and the alkanes) are substantially lower compared to the yield from BVOCs. Because these AVOCs have long lifetimes, the concentration of AVOC would need to

Formatted: Font color: Auto

Formatted: Font color: Auto

Formatted: Font color: Auto

Formatted: Font color: Auto

1 be substantially higher than BVOC to dominate the HCHO or CHOCHO budget. This is not
2 likely in most of the SE US. However, AVOCs can dominate chemistry in O&NG production
3 areas (Katzenstein et al., 2003; Edwards et al., 2014) and may be relatively more important in the
4 winter when BVOC emissions are low or in areas with less vegetation. Alkanes and ethene
5 produce less CHOCHO per HCHO compared to all BVOCs. In contrast, ethyne, benzene, and
6 toluene produce much more CHOCHO relative to HCHO. The effect of AVOCs on R_{GF} is likely
7 dependent on the speciation of emitted AVOCs, the strength of local BVOC emissions, and any
8 direct OVOC emissions (e.g. HCHO from gas flaring). These compounding factors could make
9 global measurements of R_{GF} a convoluted diagnostic for assessing the influence VOC
10 composition of AVOC emissions on ozone production a given area. different airmasses,

Formatted: Font color: Auto

11 3.5 Comparison with satellite retrievals

12 While ideally 2013 OMI retrievals would be used in this analysis, the satellite has experienced
13 severe degradation such that quantitative CHOCHO is not easily determined. Only the 2007
14 retrievals are available at this time. One of the major conclusions reached using the SENEX in-
15 situ measurements is that in the SE US, R_{GF} is not a diagnostic of anthropogenic emissions, as
16 HCHO and CHOCHO production are dominated by isoprene oxidation. Our in situ
17 measurements also show that R_{GF} is unaffected by NO_x and OH (Section 3.3). Therefore, as long
18 as isoprene is the dominant VOC for HCHO and CHOCHO production in the SE US in both
19 2007 and 2013, the comparison between 2007 satellite and 2013 in situ R_{GF} remains valid. Both
20 this work and analysis of the previous 1995 Nashville/Middle Tennessee Ozone Study (Le et al.,
21 1998) find isoprene to be the dominant HCHO source. Interannual variability of summertime
22 isoprene emissions is estimated to be between 8 and 18% for the contiguous U.S. during the
23 summers (Tawfik et al., 2012). Therefore, it is likely that isoprene is also the dominant OVOC
24 source in 2007.

25 When comparing flight-based observations with satellite retrievals, it is important to consider the
26 inherently different information these two measurements provide. Comparisons between column-
27 integrated satellite retrievals and single-altitude measurements are only valid if the point
28 measurements represent the monthlyseasonal mean of the behavior of the vertical column as a
29 whole. To examine any effect of vertical structure distribution of HCHO and CHOCHO on

Formatted: Font color: Auto

Formatted: Font color: Auto

Formatted: Font color: Auto

1 satellite observations of R_{GF} , we investigate the campaign average vertical profiles of both
2 OVOCs, and R_{GF} calculated from those averages (Fig. 8). Both OVOCs show the expected
3 decrease in concentration with altitude; however, the relative difference between boundary layer
4 and free troposphere mixing ratios is greater for HCHO. ~~Between 1 and 3 km, HCHO decreases~~
5 ~~by 76%, while CHOCHO decreases by only 57%.~~ This gives rise to a small increase in R_{GF} ~~with~~
6 ~~altitude in the free troposphere. A higher free tropospheric R_{GF} was also observed in the 1995~~
7 ~~Nashville/Middle Tennessee Ozone Study (Lee et al., 1998).~~

8 ~~At high altitudes~~ While R_{GF} is typically slightly higher in the free troposphere than the boundary
9 layer, no clear altitude dependence in R_{GF} is observed within the boundary layer (Figure 8c,
10 altitudes less than 2 km, and figure S4 for individual profiles). In the free troposphere, CHOCHO
11 measurements are below the detection limit (23 ppt at 3.25 km, detection limit = 32 ppt/5s). The
12 observed variability in R_{GF} at high altitudes can largely be attributed to noise in the CHOCHO
13 measurements at such low concentrations. ~~It is also important to consider~~ Because the possibility
14 ~~of a positive bias~~ uncertainty in CHOCHO measurements at low mixing ratios concentrations
15 from measurement precision is typically greater than that from measurement accuracy, we take
16 (Measured CHOCHO – 32 ppt) as the lower limit of CHOCHO as measured by ACES. If
17 measurements are positively biased by as little as 16 ppt, which is within this range of
18 uncertainty, corrected data would not demonstrate an increase in R_{GF} with altitude.

19 If the difference in ~~OVOC~~ HCHO and CHOCHO vertical structures is not a measurement artifact,
20 the cause of the increase in R_{GF} ~~with altitude~~ in the free troposphere is unclear. VOC precursors
21 with longer lifetimes that reach the free troposphere could preferentially form CHOCHO;
22 however, all species of measured VOCs exhibit a similar steep decrease in concentration at high
23 altitudes. Alternatively, the lifetimes of CHOCHO and HCHO could vary with altitude in such a
24 way that HCHO concentrations show a more steep vertical dependence. However, this is
25 unlikely as the photolysis and reaction with OH play nearly identical roles in the relative loss
26 processes of the ~~OVOCs~~ two OVOCs. Li et al. (2014) inferred different mixing layer heights for
27 the two OVOCs. They calculated that the lifetime of isoprene was shorter than the typical
28 boundary layer mixing time, and therefore hypothesized that HCHO production happened earlier
29 (i.e. at lower altitudes) than CHOCHO production. In contrast, we see that the boundary layer is
30 typically uniformly mixed with respect to HCHO and CHOCHO, potentially signifying the

Formatted: Font color: Auto

lifetime of the two OVOCs is longer than the boundary layer mixing time. Therefore, the time dependence of HCHO and CHOCHO production is unlikely to be the underlying cause of the difference in R_{GF} observed in the free troposphere. Finally, heterogeneous oxidation of aerosols has been proposed as a source of CHOCHO and other OVOCs in the free troposphere (Volkamer et al., 2015). No specific source of sufficient magnitude has been identified, but processes which release glyoxal, such as the ozonolysis of fatty acids (Zhou et al. 2014), would be potential candidates. Any such source would need to produce glyoxal in excess over formaldehyde.

Regardless of cause of the ~~increasing~~ higher relative R_{GF} in the free troposphere, because the boundary layer contains the majority of HCHO and CHOCHO, the ~~column-integrated~~ R_{GF} ~~between 0~~ calculated from in situ HCHO and ~~6.5 km~~ CHOCHO vertical column densities, is only slightly higher than the average R_{GF} observed in the boundary layer (2.7% ~~column-integrated~~ calculated from Q_V , 2.0% at 900 m). A similar analysis using each local vertical profile measurement rather than the campaign average vertical ~~profile~~ profiles yields the same conclusions. Table 3 lists the R_{GF} observed in the boundary layer and the R_{GF} calculated from in situ HCHO and CHOCHO vertical ~~column-integrated~~ R_{GF} densities, for all profiles extending above 3 km, which were all flown in the Atlanta/Birmingham area. A map of profile locations ~~as well as the OVOC, HCHO and CHOCHO measurements,~~ and R_{GF} for each profile can be found in the supporting information (Fig. S3 and Fig. S4). In general, profiles with a smaller percentage of measurements acquired in the free troposphere do not display large difference between boundary layer and R_{GF} calculated from in situ HCHO and CHOCHO vertical ~~column-integrated~~ R_{GF} ~~is less~~ densities. Individual profile measurements and campaign-averaged data support the conclusion that ~~column-integrated~~ R_{GF} as observed by satellite retrievals should exhibit similar ranges as boundary layer observations, though a positive bias may be observed due to relatively higher CHOCHO in the free troposphere.

OMI satellite observations from June through August of ~~2006~~ 2007, over the United States are shown in Fig. 9. HCHO and CHOCHO are elevated over the SE US, where high isoprene emissions are expected to lead to increases in both OVOCs. Compared to the rest of the US, R_{GF} in this region is low. The northwest region of the US, where monoterpene emissions are high (Sakulyanontvittaya et al., 2008), demonstrates the highest R_{GF} over the US.

- Formatted: Font color: Black, German (Germany)
- Formatted: Font color: Auto
- Formatted: Font color: Auto, Subscript
- Formatted: Font color: Auto

1 To compare satellite and flight-based observations, flight data were averaged to the 0.5° x 0.5°
2 OMI resolution. Summertime satellite retrievals and flight observations of CHOCHO v. HCHO
3 show similar correlations, with $r^2 \sim 0.4$. (Fig. 10 and Table 4). The satellite average R_{GF} is ~0.6
4 percentage points higher than flight-based observations gridded to the same resolution. While
5 this cannot be explained by the error and standard deviation of the gridded SENEX data and the
6 uncertainty in the vertical column vedsdensities, this percentage is much smaller than the
7 previous discrepancies between satellite and point-based measurements (DiGangi et al., 2012).

8 Figure 11 shows that while there is no correlation between satellite and flight R_{GF} ($r^2 = 0.003$),
9 the range of observed values are in good agreement (1.5-4%). Seasonal averages of R_{GF} from
10 satellite retrievals are less likely to reflect extreme values and high-emission events compared to
11 flight data, therefore high correlation is not anticipated at this time scale. Similarly, the
12 correlation between satellite and ground HCHO ($r^2=0.15$) and CHOCHO ($r^2=0.044$) are low.

13 Satellite and flight HCHO observations show stronger correlation than CHOCHO observations
14 likely because CHOCHO aircraft measurements and satellite retrievals have higher relative
15 uncertainties than HCHO retrievals (Miller et al., 2014; González Abad et al., 2010), and in
16 situ CHOCHO measurements are close to the detection limit. The high and low values of R_{GF}
17 observed during the SENEX field campaign (June 25th and 26th flights) are not reproduced in
18 the satellite observations A comparison of average BVOC emissions and O&NG production
19 activity during the summer of 2007 and June 2013 would be needed to demonstrate that satellite
20 R_{GF} would be expected to show similar deviations from its average value. Furthermore, small
21 scale variation in satellite R_{GF} is mostly associated with noise, such that retrievals shown cannot
22 distinguish the local influences (i.e. the Kisatchie National forest).

23 Besides the new global CHOCHO retrieval method, one key distinction between this
24 comparison and comparisons in previous studies (i.e., DiGangi et al., 2010) is the use of satellite
25 retrievals for only the summer observational period rather the annual averages. Ground and flight
26 based measurements are typically performed in the summer, when BVOC emissions are high.
27 Therefore, point-based measurements are may be biased to display the influence of BVOC
28 emissions on R_{GF} . For example, this could mean that in regions with strong isoprene emissions,
29 ground-based R_{GF} was biased lower than the annual averages with which they were compared.

Formatted: Font color: Auto

Formatted: Font color: Auto

Formatted: English (United States)

Formatted: Font color: Auto

1
2
3
4
5
6
7
8
9
10
11
12
13
14
15
16
17
18
19
20
21
22
23
24
25
26
27
28
29

4 Conclusions: Can R_{GF} be used as a global indicator of VOC speciation?

Overall, the flight-based measurements presented here show that R_{GF} is indicative of VOC speciation in select situations. High R_{GF} (>3%) is consistently observed in areas with high monoterpene emissions, and low R_{GF} (<2.5%) is associated with strong isoprene emissions. No consistent influence of AVOC or ~~NO_x~~NO_x emissions on the background R_{GF} was observed, likely because biogenic VOC emission strength determines R_{GF} in the SE US. The previously observed quick and short (2-5 min) increase in R_{GF} in DiGangi et al. (2010) may have been a result of extremely fresh emissions (e.g., diesel trucks emit at a rate of CHOCHO/HCHO = 9.4% (Schauer et al., 1999), and not indicative of larger scale changes in dominant VOC speciation. Emissions associated with oil and gas production areas can cause R_{GF} to deviate from the values observed over their background levels. However, the absolute value of R_{GF} in such regions is likely dependent on background BVOC emissions, speciation of AVOCs, and any direct OVOC emissions.

Compared to previous literature, absolute values of flight-based R_{GF} are in better agreement with satellite observations using the new ~~glyoxal~~CHOCHO retrieval algorithms. While time resolution plays a large role in direct comparisons of point-based measurements and satellite retrievals, the trend of high R_{GF} over areas with monoterpenes and low R_{GF} over areas with isoprene is broadly in agreement for the two platforms. With these trends validated by ground measurements, R_{GF} based on satellite retrievals may be useful as a diagnostic of BVOC emissions. As these retrievals become available at higher time and spatial resolution, R_{GF} can be used to help identify the speciation of VOCs leading to secondary pollutant formation on a regional scale.

Acknowledgements

The authors would like to acknowledge contribution from all members of the SENEX flight and science teams. Funding was provided by U.S. EPA-Science to Achieve Results (STAR) program- Grant 83540601. This research has not been subjected to any EPA review and therefore does not necessarily reflect the views of the Agency, and no official endorsement

Formatted: Font color: Auto

Formatted: Font color: Auto

Formatted: Font color: Auto

1 should be inferred. J. Kaiser acknowledges support from NASA Headquarters under the NASA
2 Earth and Space Science Fellowship Program - Grant NNX14AK97H. This work was also
3 supported as part of the NASA Aura Science Team.

5 **References**

6 Bey, I., Jacob, D. J., Yantosca, R. M., Logan, J. A., Field, B. D., Fiore, A. M., Li, Q. B., Liu, H.
7 G. Y., Mickley, L. J., and Schultz, M. G.: Global modeling of tropospheric chemistry with
8 assimilated meteorology: Model description and evaluation, *J. Geophys. Res.-Atmos*, 106,
9 23073-23095, 10.1029/2001jd000807, 2001.

10 Cazorla, M., Wolfe, G. M., Bailey, S. A., Swanson, A. K., Arkinson, H. L., and Hanisco, T. F.: A
11 new airborne laser-induced fluorescence instrument for in situ detection of Formaldehyde
12 throughout the troposphere and lower stratosphere, *Atmos. Meas. Tech. Discuss.*, 7, 8359-8391,
13 10.5194/amtd-7-8359-2014, 2014.

14 Christian, T. J., Kleiss, B., Yokelson, R. J., Holzinger, R., Crutzen, P. J., Hao, W. M., Saharjo, B.
15 H., and Ward, D. E.: Comprehensive laboratory measurements of biomass-burning emissions. 1.
16 Emissions from Indonesian, African, and other fuels, *J. Geophys. Res.*, 108, ACH3-1-13,
17 10.1029/2002jd003704, 2003.

18 de Gouw, J., and Warneke, C.: Measurements of volatile organic compounds in the earths
19 atmosphere using proton-transfer-reaction mass spectrometry, *Mass Spectrom. Rev.*, 26, 223-
20 257, 10.1002/mas.20119, 2007.

21 DiGangi, J., Boyle, E., Karl, T., Harley, P., Turnipseed, A., Kim, S., Cantrell, C., Maudlin, R.,
22 Zheng, W., Flocke, F., Hall, S., Ullmann, K., Nakashima, Y., Paul, J., Wolfe, G., Desai, A.,
23 Kajii, Y., Guenther, A., and Keutsch, F.: First direct measurements of formaldehyde flux via
24 eddy covariance: implications for missing in-canopy formaldehyde sources, *Atmos. Chem.*
25 *Phys.*, 11, 10565-10578, 10.5194/acp-11-10565-2011, 2011.

26 DiGangi, J., Henry, S., Kammrath, A., Boyle, E., Kaser, L., Schnitzhofer, R., Graus, M.,
27 Turnipseed, A., Park, J., Weber, R., Hornbrook, R., Cantrell, C., Maudlin, R., Kim, S.,
28 Nakashima, Y., Wolfe, G., Kajii, Y., Apel, E., Goldstein, A., Guenther, A., Karl, T., Hansel, A.,

1 and Keutsch, F.: Observations of glyoxal and formaldehyde as metrics for the anthropogenic
2 impact on rural photochemistry, *Atmos. Chem. Phys.*, 12, 9529-9543, 10.5194/acp-12-9529-
3 2012, 2012.

4 Edwards, P. M., Brown, S. S., Roberts, J. M., Ahmadov, R., Banta, R. M., deGouw, J. A., Dube,
5 W. P., Field, R. A., Flynn, J. H., Gilman, J. B., Graus, M., Helmig, D., Koss, A., Langford, A.
6 O., Lefer, B. L., Lerner, B. M., Li, R., Li, S.-M., McKeen, S. A., Murphy, S. M., Parrish, D. D.,
7 Senff, C. J., Soltis, J., Stutz, J., Sweeney, C., Thompson, C. R., Trainer, M. K., Tsai, C., Veres,
8 P. R., Washenfelder, R. A., Warneke, C., Wild, R. J., Young, C. J., Yuan, B., and Zamora, R.:
9 High winter ozone pollution from carbonyl photolysis in an oil and gas basin, *Nature*, 514, 351-
10 354, 10.1038/nature13767, 2014.

11 Fortems-Cheiney, A., Chevallier, F., Pison, I., Bousquet, P., Saunois, M., Szopa, S., Cressot, C.,
12 Kurosu, T. P., Chance, K., and Fried, A.: The formaldehyde budget as seen by a global-scale
13 multi-constraint and multi-species inversion system, *Atmos. Chem. Phys.*, 12, 6699-6721,
14 10.5194/acp-12-6699-2012, 2012.

15 Fu, T.-M., Jacob, D. J., Wittrock, F., Burrows, J. P., Vrekoussis, M., and Henze, D. K.: Global
16 budgets of atmospheric glyoxal and methylglyoxal, and implications for formation of secondary
17 organic aerosols, *J. Geophys. Res.-Atmos*, 113, 10.1029/2007jd009505, 2008.

18 Garcia, A. R., Volkamer, R., Molina, L. T., Molina, M. J., Samuelson, J., Mellqvist, J., Galle, B.,
19 Herndon, S. C., and Kolb, C. E.: Separation of emitted and photochemical formaldehyde in
20 Mexico City using a statistical analysis and a new pair of gas-phase tracers, *Atmos. Chem. Phys.*,
21 6, 4545-4557, 2006.

22 Gilman, J. B., Lerner, B. M., Kuster, W. C., and de Gouw, J. A.: Source Signature of Volatile
23 Organic Compounds from Oil and Natural Gas Operations in Northeastern Colorado, *Environ.*
24 *Sci. Technol.*, 47, 1297-1305, 10.1021/es304119a, 2013.

25 Goldstein, A. H., and Galbally, I. E.: Known and unexplored organic constituents in the earth's
26 atmosphere, *Environ. Sci. Technol.*, 41, 1514-1521, 10.1021/es072476p, 2007.

27 González Abad, G., Liu, X., Chance, K., Wang, H., Kurosu, T. P., and Suleiman, R.: Updated
28 [Smithsonian Astrophysical Observatory Ozone Monitoring Instrument \(SAO OMI\)](#)

Formatted: Font color: Auto

Formatted: Font color: Auto

1 formaldehyde retrieval, Atmos. Meas. Tech. ~~Discuss., 7, 1-31, 8, 19-32~~, 10.5194/~~amt-7-1-~~
2 ~~2014, 2014~~amt-8-19-2015, 2015.

3 Greenberg, J. P., Friedli, H., Guenther, A. B., Hanson, D., Harley, P., and Karl, T.: Volatile
4 organic emissions from the distillation and pyrolysis of vegetation, Atmos. Chem. Phys., 6, 81-
5 91, 2006.

6 Guenther, A., Hewitt, C. N., Erickson, D., Fall, R., Geron, C., Graedel, T., Harley, P., Klinger,
7 L., Lerdau, M., McKay, W. A., Pierce, T., Scholes, B., Steinbrecher, R., Tallamraju, R., Taylor,
8 J., and Zimmerman, P.: A global model of natural volatile compound emissions, J. Geophys.
9 Res.-Atmos, 100, 8873-8892, 10.1029/94jd02950, 1995.

10 Hays, M. D., Geron, C. D., Linna, K. J., Smith, N. D., and Schauer, J. J.: Speciation of gas-phase
11 and fine particle emissions from burning of foliar fuels, Environ. Sci. Technol., 36, 2281-2295,
12 10.1021/es0111683, 2002.

13 Holzinger, R., Warneke, C., Hansel, A., Jordan, A., Lindinger, W., Scharffe, D. H., Schade, G.,
14 and Crutzen, P. J.: Biomass burning as a source of formaldehyde, acetaldehyde, methanol,
15 acetone, acetonitrile, and hydrogen cyanide, Geophys. Res. Lett., 26, 1161-1164,
16 10.1029/1999gl900156, 1999.

17 Hottle, J., Huisman, A., Digangi, J., Kammrath, A., Galloway, M., Coens, K., and Keutsch, F.: A
18 Laser Induced Fluorescence-Based Instrument for In-Situ Measurements of Atmospheric
19 Formaldehyde, Environ. Sci. Technol., 43, 790-795, 10.1021/es801621f, 2009.

20 Jenkin, M., Saunders, S., and Pilling, M.: The tropospheric degradation of volatile organic
21 compounds: A protocol for mechanism development, Atmos. Environ., 31, 81-104,
22 10.1016/S1352-2310(96)00105-7, 1997.

23 Kaiser, J., Li, X., Tillmann, R., Acir, I., Holland, F., Rohrer, F., Wegener, R., and Keutsch, F. N.:
24 Intercomparison of Hantzsch and fiber-laser-induced-fluorescence formaldehyde measurements,
25 Atmos. Meas. Tech., 7, 1571-1580, 10.5194/amt-7-1571-2014, 2014.

26 Katzenstein, A. S., Doezema, L. A., Simpson, I. J., Balke, D. R., and Rowland, F. S.: Extensive
27 regional atmospheric hydrocarbon pollution in the southwestern United States, P. Natl. Acad.
28 Sci. USA, 100, 11975-11979, 10.1073/pnas.1635258100, 2003.

Formatted: Font color: Auto

Formatted: Font color: Auto

1 Kesselmeier, J., Bode, K., Hofmann, U., Muller, H., Schafer, L., Wolf, A., Ciccioli, P.,
2 Brancaleoni, E., Cecinato, A., Frattoni, M., Foster, P., Ferrari, C., Jacob, V., Fugit, J. L., Dutaur,
3 L., Simon, V., and Torres, L.: Emission of short chained organic acids, aldehydes and
4 monoterpenes from *Quercus ilex* L. and *Pinus pinea* L. in relation to physiological activities,
5 carbon budget and emission algorithms, *Atmos. Environ.*, 31, 119-133, 10.1016/s1352-
6 2310(97)00079-4, 1997.

7 [Lee, Y. N., Zhou, X., Kleinman, L. I., Nunnermacker, L. J., Springston, S. R., Daum, P. H.,](#)
8 [Newman, L., Keigley, W. G., Holdren, M. W., Spicer, C. W., Young, V., Fu, B., Parrish, D. D.,](#)
9 [Holloway, J., Williams, J., Roberts, J. M., Ryerson, T. B., and Fehsenfeld, F. C.: Atmospheric](#)
10 [chemistry and distribution of formaldehyde and several multioxygenated carbonyl compounds](#)
11 [during the 1995 Nashville Middle Tennessee Ozone Study, *J. Geophys. Res.*, 103, 22449-22462,](#)
12 [10.1029/98JD01251, 1998.](#)

13 [Levelt, P. F., Van den Oord, G. H. J., Dobber, M. R., Malkki, A., Visser, H., de Vries, J.,](#)
14 [Stammes, P., Lundell, J. O. V., and Saari, H.: The Ozone Monitoring Instrument, *IEEE Trans.*](#)
15 [Geosci. Remote Sens.](#), 44, 1093-1101, 10.1109/tgrs.2006.872333, 2006.

16 Li, X., Rohrer, F., Brauers, T., Hofzumahaus, A., Lu, K., Shao, M., Zhang, Y. H., and Wahner,
17 A.: Modeling of HCHO and CHOCHO at a semi-rural site in southern China during the PRIDE-
18 PRD2006 campaign, *Atmos. Chem. Phys.*, 14, 12291-12305, 10.5194/acp-14-12291-2014, 2014.

19 Liu, X., Chance, K., Sioris, C. E., Kurosu, T. P., Spurr, R. J. D., Martin, R. V., Fu, T. M., Logan,
20 J. A., Jacob, D. J., Palmer, P. I., Newchurch, M. J., Megretskaia, I. A., and Chatfield, R. B.: First
21 directly retrieved global distribution of tropospheric column ozone from GOME: Comparison
22 with the GEOS-CHEM model, *J. Geophys. Res.-Atmos.*, 111, 10.1029/2005jd006564, 2006.

23 MacDonald, S. M., Oetjen, H., Mahajan, A. S., Whalley, L. K., Edwards, P. M., Heard, D. E.,
24 Jones, C. E., and Plane, J. M. C.: DOAS measurements of formaldehyde and glyoxal above a
25 south-east Asian tropical rainforest, *Atmos. Chem. Phys.*, 12, 5949-5962, 10.5194/acp-12-5949-
26 2012, 2012.

27 Mao, J., Paulot, F., Jacob, D. J., Cohen, R. C., Crouse, J. D., Wennberg, P. O., Keller, C. A.,
28 Hudman, R. C., Barkley, M. P., and Horowitz, L. W.: Ozone and organic nitrates over the

Formatted: Font color: Auto

1 eastern United States: Sensitivity to isoprene chemistry, *J. Geophys. Res.-Atmos*, 118, 11256-
2 11268, 10.1002/jgrd.50817, 2013.

3 Marais, E. A., Jacob, D. J., Kurosu, T. P., Chance, K., Murphy, J. G., Reeves, C., Mills, G.,
4 Casadio, S., Millet, D. B., Barkley, M. P., Paulot, F., and Mao, J.: Isoprene emissions in Africa
5 inferred from OMI observations of formaldehyde columns, *Atmos. Chem. Phys.*, 12, 6219-6235,
6 10.5194/acp-12-6219-2012, 2012.

7 McDonald, J. D., Zielinska, B., Fujita, E. M., Sagebiel, J. C., Chow, J. C., and Watson, J. G.:
8 Fine particle and gaseous emission rates from residential wood combustion, *Environ. Sci.*
9 *Technol.*, 34, 2080-2091, 10.1021/es9909632, 2000.

10 Miller, C. C., Abad, G. G., Wang, H., Liu, X., Kurosu, T., Jacob, D. J., and Chance, K.: Glyoxal
11 retrieval from the Ozone Monitoring Instrument, *Atmos. Meas. Tech.* ~~*Discuss.*~~, 7, ~~6065-~~
12 ~~61123891-3907~~, 10.5194/~~amt~~~~amt~~-7-~~60653891~~-2014, 2014.

13 Palmer, P. I., Abbot, D. S., Fu, T.-M., Jacob, D. J., Chance, K., Kurosu, T. P., Guenther, A.,
14 Wiedinmyer, C., Stanton, J. C., Pilling, M. J., Pressley, S. N., Lamb, B., and Sumner, A. L.:
15 Quantifying the seasonal and interannual variability of North American isoprene emissions using
16 satellite observations of the formaldehyde column, *J. Geophys. Res.-Atmos*, 111,
17 10.1029/2005jd006689, 2006.

18 Pikelnaya, O., Flynn, J. H., Tsai, C., and Stutz, J.: Imaging DOAS detection of primary
19 formaldehyde and sulfur dioxide emissions from petrochemical flares, *J. Geophys. Res.-Atmos*,
20 118, 8716-8728, 10.1002/jgrd.50643, 2013.

21 Pollack, I. B., Lerner, B. M., and Ryerson, T. B.: Evaluation of ultraviolet light-emitting diodes
22 for detection of atmospheric NO₂ by photolysis - chemiluminescence, *J. Atmos. Chem.*, 65, 111-
23 125, 10.1007/s10874-011-9184-3, 2010.

24 Rasmusse, R. A.: What do the hydrocarbons from trees contribute to air pollution?, *J. Air Pollut.*
25 *Contr. Assoc.*, 22, 537-543, 1972.

26 Rivera-Rios, J. C., Nguyen, T. B., Crouse, J. D., Jud, W., St. Clair, J. M., Mikoviny, T.,
27 Gilman, J. B., Lerner, B. M., Kaiser, J. B., de Gouw, J., Wisthaler, A., Hansel, A., Wennberg, P.
28 O., Seinfeld, J. H., and Keutsch, F. N.: Conversion of hydroperoxides to carbonyls in field and

Formatted: Font color: Auto

Formatted: Font color: Auto

Formatted: Font color: Auto

Formatted: Font color: Auto

1 laboratory instrumentation: observational bias in diagnosing pristine versus anthropogenically-
2 controlled atmospheric chemistry, *Geophys. Res. Lett.*, 2014GL061919,
3 10.1002/2014GL061919, 2014.

4 Rohrer, F., Lu, K. D., Hofzumahaus, A., Bohn, B., Brauers, T., Chang, C. C., Fuchs, H., Haseler,
5 R., Holland, F., Hu, M., Kita, K., Kondo, Y., Li, X., Lou, S. R., Oebel, A., Shao, M., Zeng, L.
6 M., Zhu, T., Zhang, Y. H., and Wahner, A.: Maximum efficiency in the hydroxyl-radical-based
7 self-cleansing of the troposphere, *Nature Geoscience*, 7, 559-563, 10.1038/ngeo2199, 2014.

8 Ryerson, T. B., Williams, E. J., and Fehsenfeld, F. C.: An efficient photolysis system for fast-
9 response NO₂ measurements, *J. Geophys. Res.-Atmos*, 105, 26447-26461,
10 10.1029/2000jd900389, 2000.

11 Sakulyanontvittaya, T., Duhl, T., Wiedinmyer, C., Helmig, D., Matsunaga, S., Potosnak, M.,
12 Milford, J., and Guenther, A.: Monoterpene and sesquiterpene emission estimates for the United
13 States, *Environ. Sci. Technol.*, 42, 1623-1629, 10.1021/es702274e, 2008.

14 Saunders, S., Jenkin, M., Derwent, R., and Pilling, M.: Protocol for the development of the
15 Master Chemical Mechanism, MCM v3 (Part A): tropospheric degradation of non-aromatic
16 volatile organic compounds, *Atmos. Chem. Phys.*, 3, 161-180, 2003.

17 Schauer, J. J., Kleeman, M. J., Cass, G. R., and Simoneit, B. R. T.: Measurement of emissions
18 from air pollution sources. 2. C-1 through C-30 organic compounds from medium duty diesel
19 trucks, *Environ. Sci. Technol.*, 33, 1578-1587, 10.1021/es980081n, 1999.

20 Stammes, P., Sneep, M., De Haan, J. F., Veefkind, J. P., Wang, P., and Levelt, P. F.: Effective
21 cloud fractions from the Ozone Monitoring Instrument: Theoretical framework and validation, *J.*
22 *Geophys. Res.-Atmos*, 113, 10.1029/2007jd008820, 2008.

23 [Stavrakou, T., Muller, J.-F., De Smedt, I., Van Roozendael, M., Kanakidou, M., Vrekoussis, M.,](#)
24 [Wittrock, F., Richter, A., and Burrows, J. P.: The continental source of glyoxal estimated by the](#)
25 [synergistic use of spaceborne measurements and inverse modelling, *Atmos. Chem. Phys.*, 9,](#)
26 [8431-8446, 10.5194/acp-9-8431-2009, 2009.](#)

1 [Tawfik, A. B., Stöckli, R., Goldstein, A., Pressley, S., and Steiner, A. L.: Quantifying the](#)
2 [contribution of environmental factors to isoprene flux interannual variability, *Atmos. Environ.*,](#)
3 [54, 216–224, 10.1016/j.atmosenv.2012.02.018, 2012.](#)

4 [Volkamer, R. et al., Aircraft measurements of bromine monoxide, iodine monoxide, and glyoxal](#)
5 [profiles in the tropics: comparison with ship-based and in situ measurements, *Atmos. Meas.*](#)
6 [Tech. Discuss.](#), 8, 623-687, 10.5194/amtd-8-623-2015, 2015.

7 Vrekoussis, M., Wittrock, F., Richter, A., and Burrows, J. P.: GOME-2 observations of
8 oxygenated VOCs: what can we learn from the ratio glyoxal to formaldehyde on a global scale?,
9 *Atmos. Chem. Phys.*, 10, 10145-10160, 10.5194/acp-10-10145-2010, 2010.

10 Washenfelder, R. A., Wagner, N. L., Dube, W. P., and Brown, S. S.: Measurement of
11 Atmospheric Ozone by Cavity Ring-down Spectroscopy, *Environ. Sci. Technol.*, 45, 2938-2944,
12 10.1021/es103340u, 2011.

13 Wiedinmyer, C., Greenberg, J., Guenther, A., Hopkins, B., Baker, K., Geron, C., Palmer, P. I.,
14 Long, B. P., Turner, J. R., Petron, G., Harley, P., Pierce, T. E., Lamb, B., Westberg, H., Baugh,
15 W., Koerber, M., and Janssen, M.: Ozarks Isoprene Experiment (OZIE): Measurements and
16 modeling of the "isoprene volcano", *J. Geophys. Res.-Atmos.*, 110, 10.1029/2005jd005800, 2005.

17 Wolfe, G., and Thornton, J.: The Chemistry of Atmosphere-Forest Exchange (CAFE) Model -
18 Part 1: Model description and characterization, *Atmos. Chem. Phys.*, 11, 77-101, 10.5194/acp-
19 11-77-2011, 2011.

20 [Zhou, S., Gonzalez, L., Leithead, A., Finewax, Z., Thalman, R., Vlasenko, A., Vagle, S., Miller,](#)
21 [L. A., Li, S.-M., Bureekul, S., Furutani, H., Uematsu, M., Volkamer, R., and Abbatt, J.:](#)
22 [Formation of gas-phase carbonyls from heterogeneous oxidation of polyunsaturated fatty acids at](#)
23 [the air-water interface and of the sea surface microlayer, *Atmos. Chem. Phys.*, 14, 1371-1384,](#)
24 [10.5194/acp-14-1371-2014, 2014.](#)

Formatted: Font color: Auto

Formatted: Font color: Auto

1 Table 1. Summary of previous published absolute values and trends of R_{GF}

Reference	Method	R_{GF} under biogenic influence (%)	R_{GF} under anthropogenic influence (%)	Trend in R_{GF} with anthropogenic influence
Vrekousiss et al. (2010)	Satellite	>4.5	<4.5	Decreasing
DiGangi et al. (2012)	LIF ^a /LIP ^b ; review of previous ground-based measurements	<2	>2.5	Increasing; independent of NO_x
MacDonald et al. (2012)	DOAS ^c ; model analysis	20-40	--	--
Li et al. (2014)	DOAS; model analysis	0.2-17		Generally increasing; depends on NO_x , OH, and physical processes
Miller et al. (2014)	Satellite	<4 (isoprene) >4 (monoterpenes)	~4	Depends on BVOC
This work	LIF/ACES ^d	<2.5(isoprene) >3 (monoterpenes)	variable	Depends on BVOC and AVOC

2 ^aLaser Induced Fluorescence (HCHO)

3 ^bLaser Induced Phosphorescence (CHOCHO)

4 ^cDifferential Optical Absorption Spectroscopy

5 ^dAirborne Cavity Enhanced Spectrometer (CHOCHO)

1 Table 2. Relative abundance of ~~OVOCs~~HCHO and CHOCHO from 1 ppb of a given precursor^a

Precursor	CHOCHO	HCHO	Ratio (%) ^b
Isoprene	0.27 ppb	4.3 ppb	6.3
α -pinene	0.31 ppb	3.6 ppb	8.6
β -pinene	0.49 ppb	3.6 ppb	14
Ethane	0.02 ppt	5.4 ppt	0.4
Ethene	586 ppt	24 ppt	4.2
Ethyne	0.91 ppt	14 ppt	1500
Propane	0.02 ppt	8.8 ppt	0.2
n-butane	1.5 ppt	140 ppt	1.1
Benzene	23 ppt	7.6 ppt	303
Toluene	103 ppt	150 ppt	69

2 ^aCalculated using a 0-D box model. See text for details.

3 ^bRatio = CHOCHO/HCHO

Formatted: Font color: Auto

1 Table 3. Comparison of column-integrated and boundary layer R_{GF}

Profile number	Boundary layer R_{GF} ^a	Column-integrated R_{GF} calculated from in situ HCHO Ω_V and CHOCHO Ω_V	Difference ^b	% of altitude range in FT ^c
1	2.7	3.2	0.6	68
2	2.2	2.6	0.4	53
3	2.7	3.4	0.7	50
4	2.0	2.1	0.1	50
5	1.7	2.1	0.4	50
6	1.9	2.2	0.3	47
7	2.4	2.2	-0.2	42
8	1.9	1.9	0.0	17
9	2.1	2.1	0.0	15
10	2.5	1.9	-0.7	15
11	2.6	2.4	-0.2	8
12	2.0	2.1	0.1	8

2 ^aObserved at 1 km

3 ^bCalculated as column-integrated R_{GF} - boundary layer R_{GF}

4 ^c~~Boundary~~ FT = Free troposphere. ~~Boundary~~ layer height determined by gradient in O_3

- Formatted: Font color: Auto

1 | Table 4. Linear fits of CHOCHO v. HCHO observations^a

Method	Slope	Intercept	r^2	Average R_{GF} (%)
Flight	0.017	0.019 ppb	0.43	2.2
Satellite	0.024	~0.016 ppb ^b (6.6×10^{13} molec/cm ²)	0.38	2.8

2 | ^aAll data are gridded to 0.5° x 0.5° resolution for orthogonal distance regression analysis. For
 3 | SENEX flight observations, all flights (including Haynesville and Fayetteville areas) are
 4 | included.

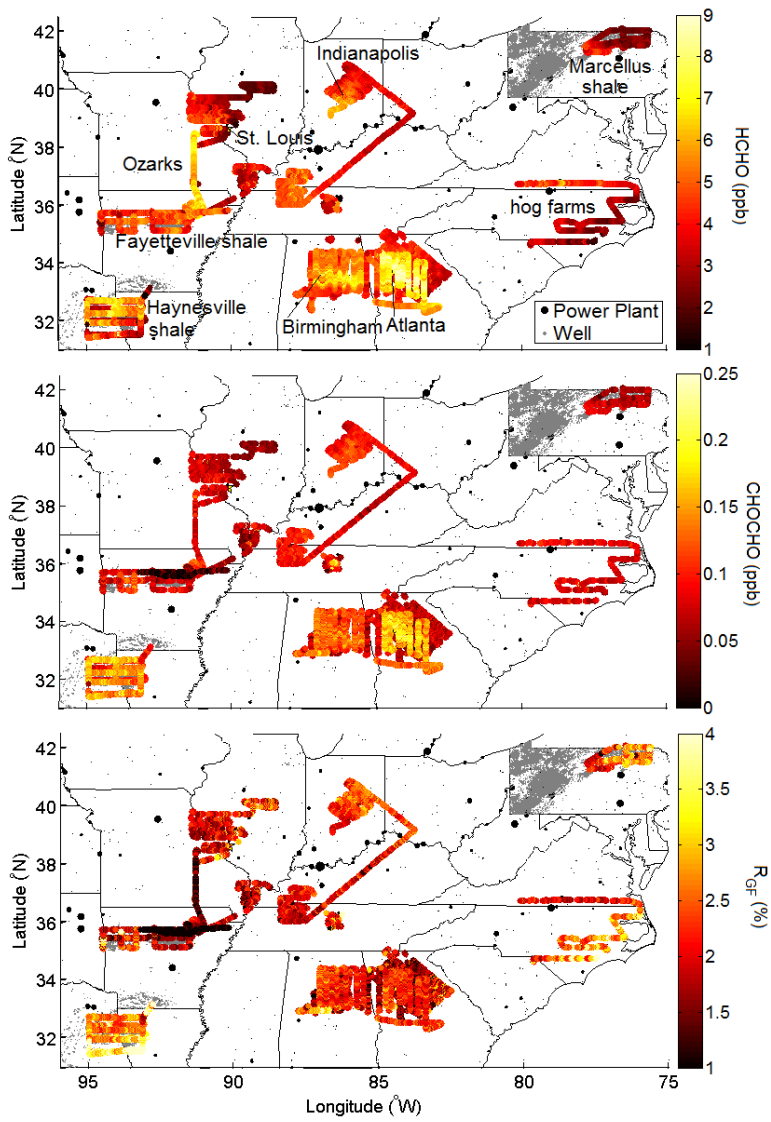
5 | ^bGround level mixing ratio was calculated assuming CHOCHO ~~is~~ and HCHO ~~are~~ contained
 6 | within a well mixed 1500 m boundary layer and an atmospheric scale height of 7.5 km.

Formatted: Font color: Auto

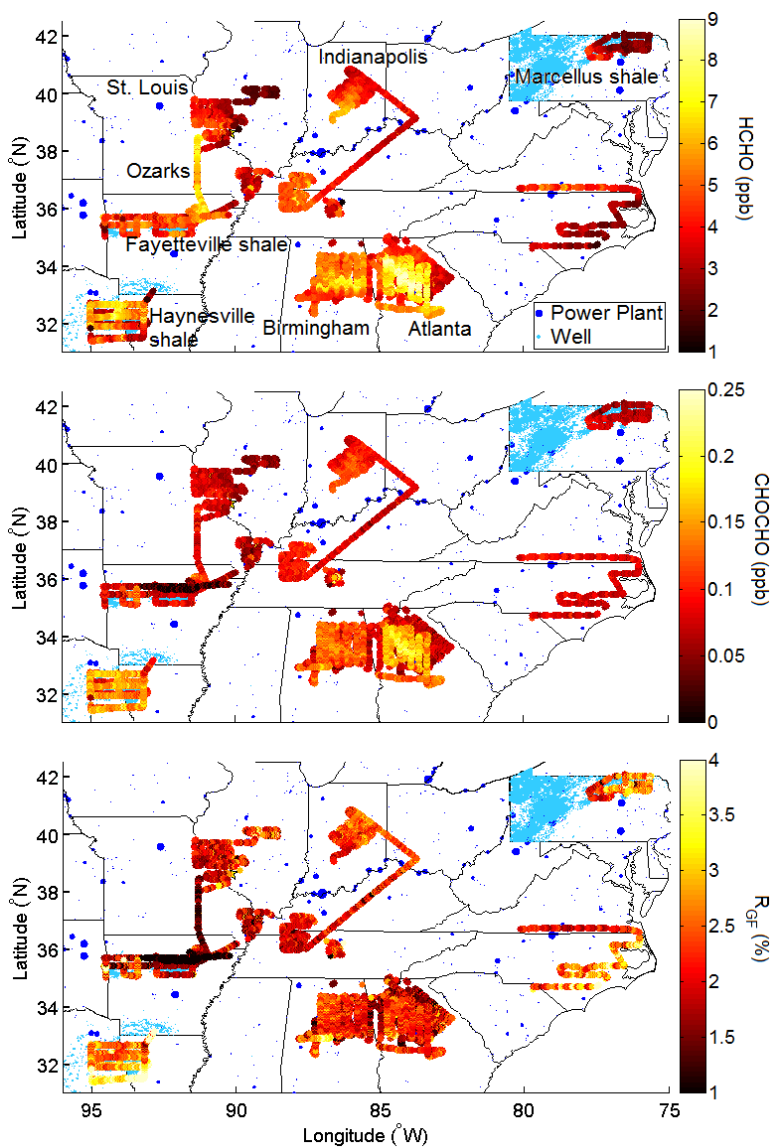
Formatted: Font color: Auto

Formatted: Font color: Auto

Formatted: Font color: Auto



Formatted: Font: 10 pt, Font color: Text 1



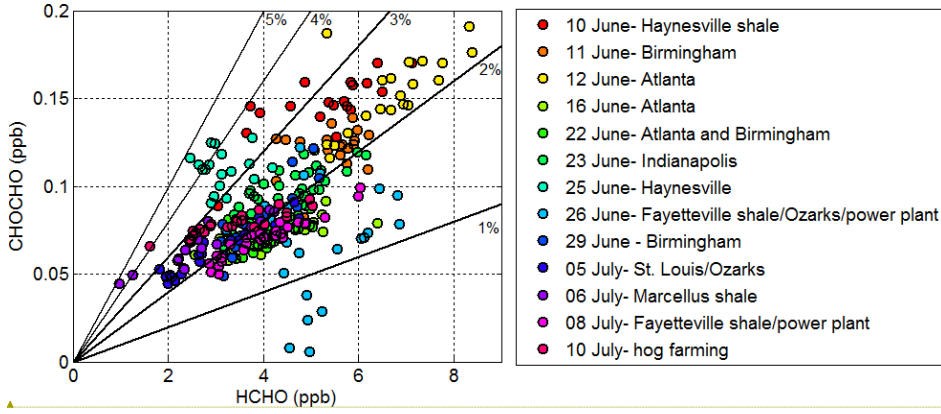
1
 2 Figure 1. Daytime flight tracks colored by HCHO, CHOCHO, and R_{GF} . Power plant markers are
 3 scaled by NO_x/NO_x emissions.

Formatted: Font color: Auto

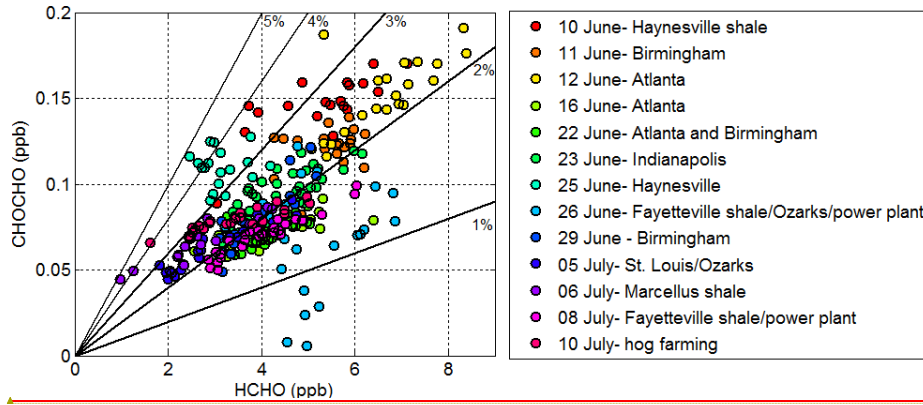
Formatted: Font color: Auto

Formatted: Font color: Auto

Formatted: Font color: Auto



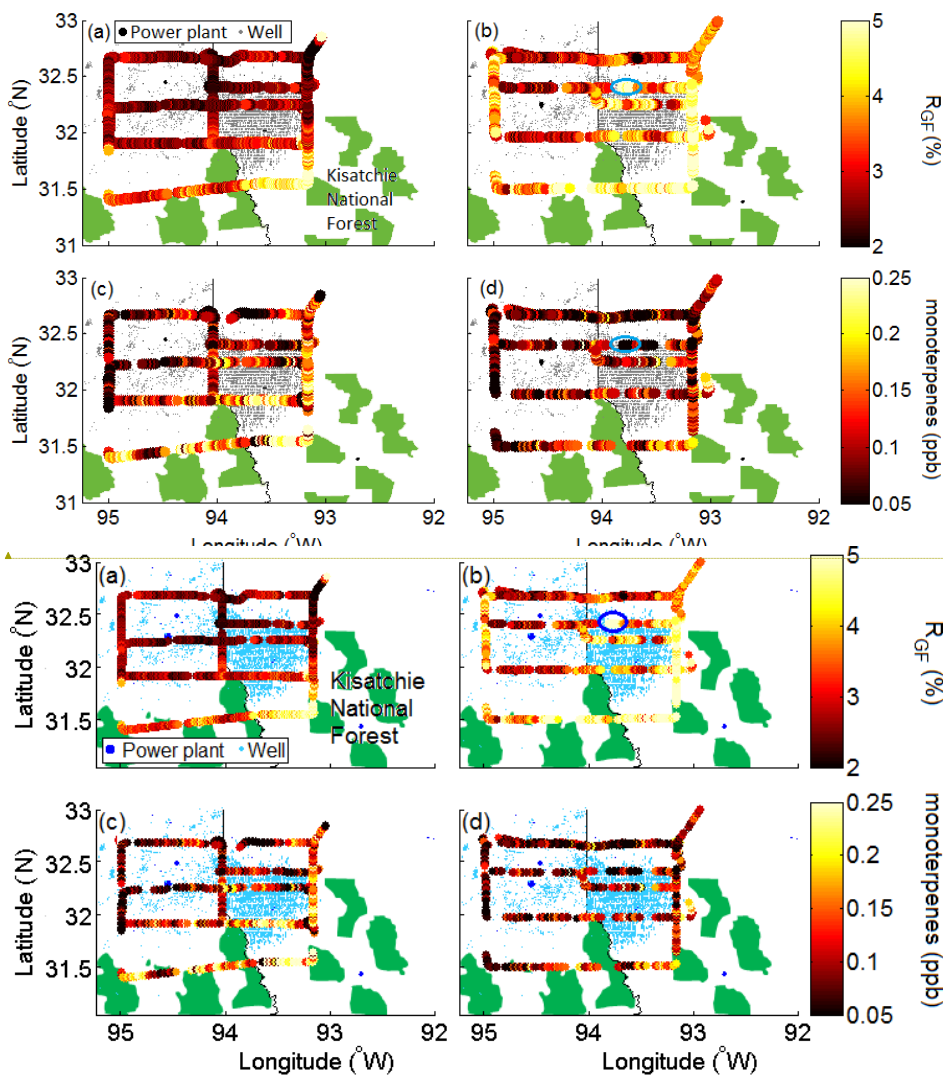
Formatted: Font color: Text 1



Formatted: Font color: Auto

Figure 2. The relationship of CHOCHO and HCHO for each flight, gridded to OMI satellite resolution. Flights with extreme values of R_{GF} include those to the Haynesville shale (~~6/10 June~~ and ~~6/25 June~~) and the Ozarks (~~6/26 June~~).

Formatted: Font color: Auto



1

2

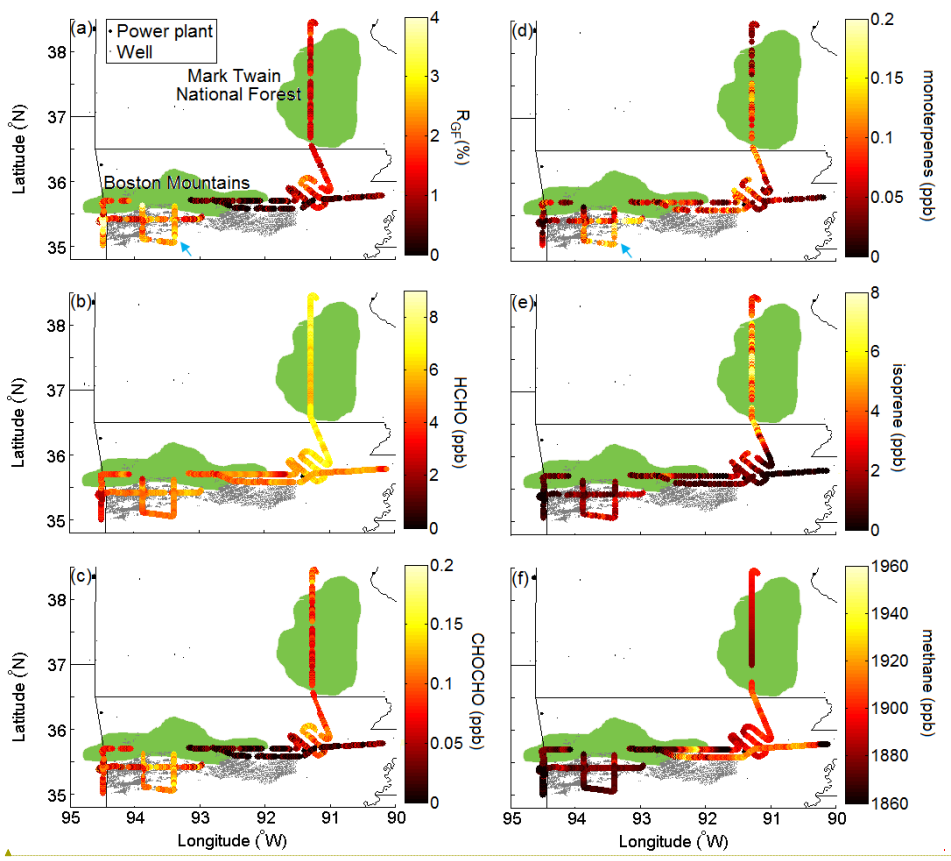
3 Figure 3. Flight tracks for 10 June 10th (a, c) 25 June 25th (b,d) over the Haynesville shale,
 4 colored by R_{GF} and the measured monoterpene mixing ratio. The southeast corner highlights
 5 high R_{GF} in a region with high monoterpene concentrations. The blue circle indicates the location
 6 of high R_{GF} discussed further in the text. Figure 5 shows meteorological and trace gas

Formatted: Font color: Text 1

Formatted: Font color: Auto

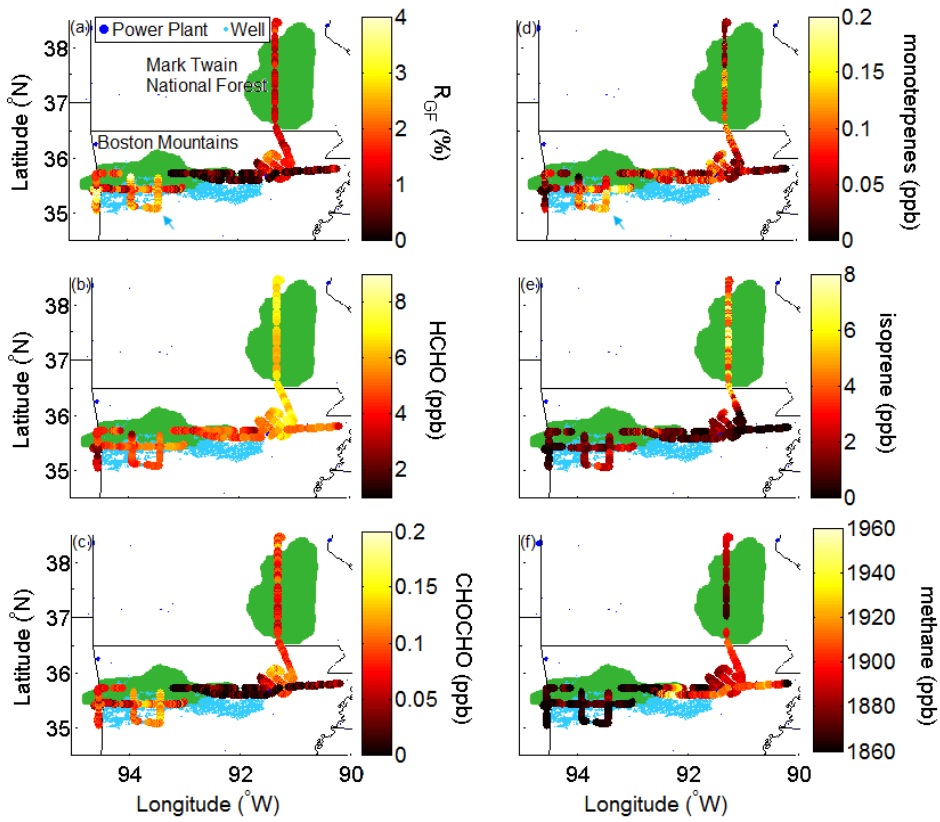
- 1 | measurements acquired at this location. National parks are shown in green, and the Kisatchie
- 2 | National Forest is labeled in (a).

Formatted: Font color: Auto



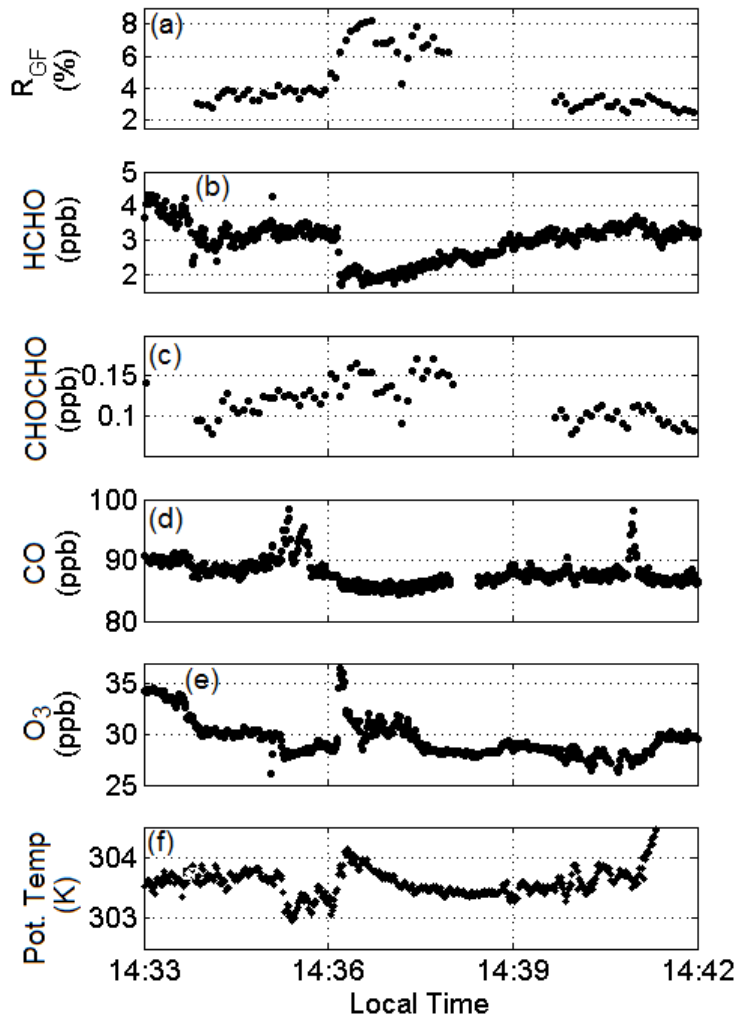
Formatted: Font color: Text 1

1

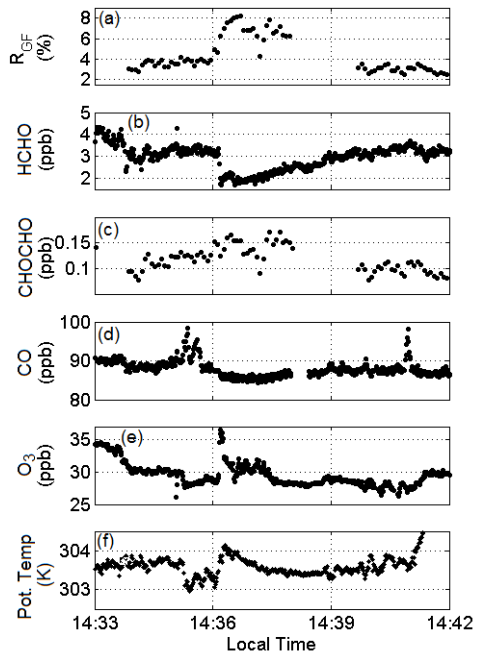


1
 2 Figure 4. Flight track for the 26 June-26th over the Fayetteville shale, the independence power
 3 plant, and the Ozarks, colored by the specified trace gas mixing ratio and R_{GF} . The blue arrow
 4 highlights the region of elevated monoterpene mixing ratios. National forests are shown in green.

Formatted: Font color: Auto



Formatted: Font color: Text 1



1

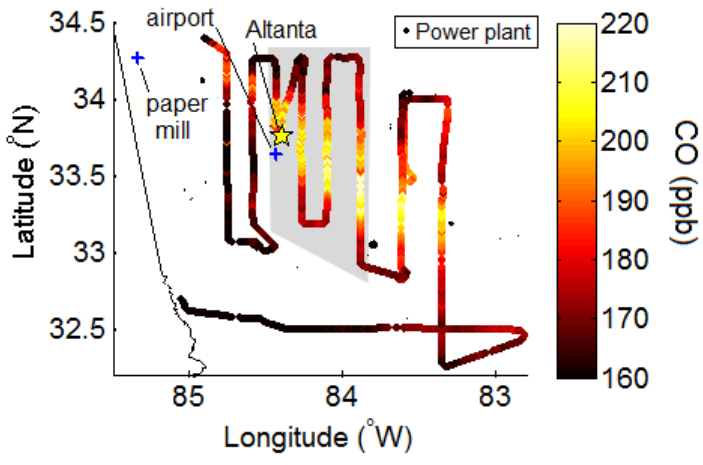
2 Figure 5. Time series of specified measurements during the rapid increase in R_{GF} observed south
 3 of Shreveport on the 25 June 25th flight (blue circle in Fig. 3). An incursion of free tropospheric
 4 air near 14:36 L.T. drives high R_{GF} .

Formatted: Font color: Auto

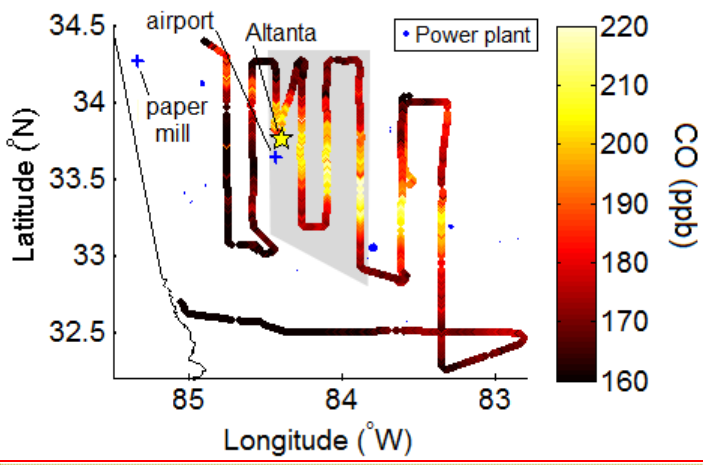
Formatted: Font color: Auto

Formatted: Font color: Auto

Formatted: Font color: Auto



Formatted: Font color: Text 1



Formatted: Font color: Auto

1

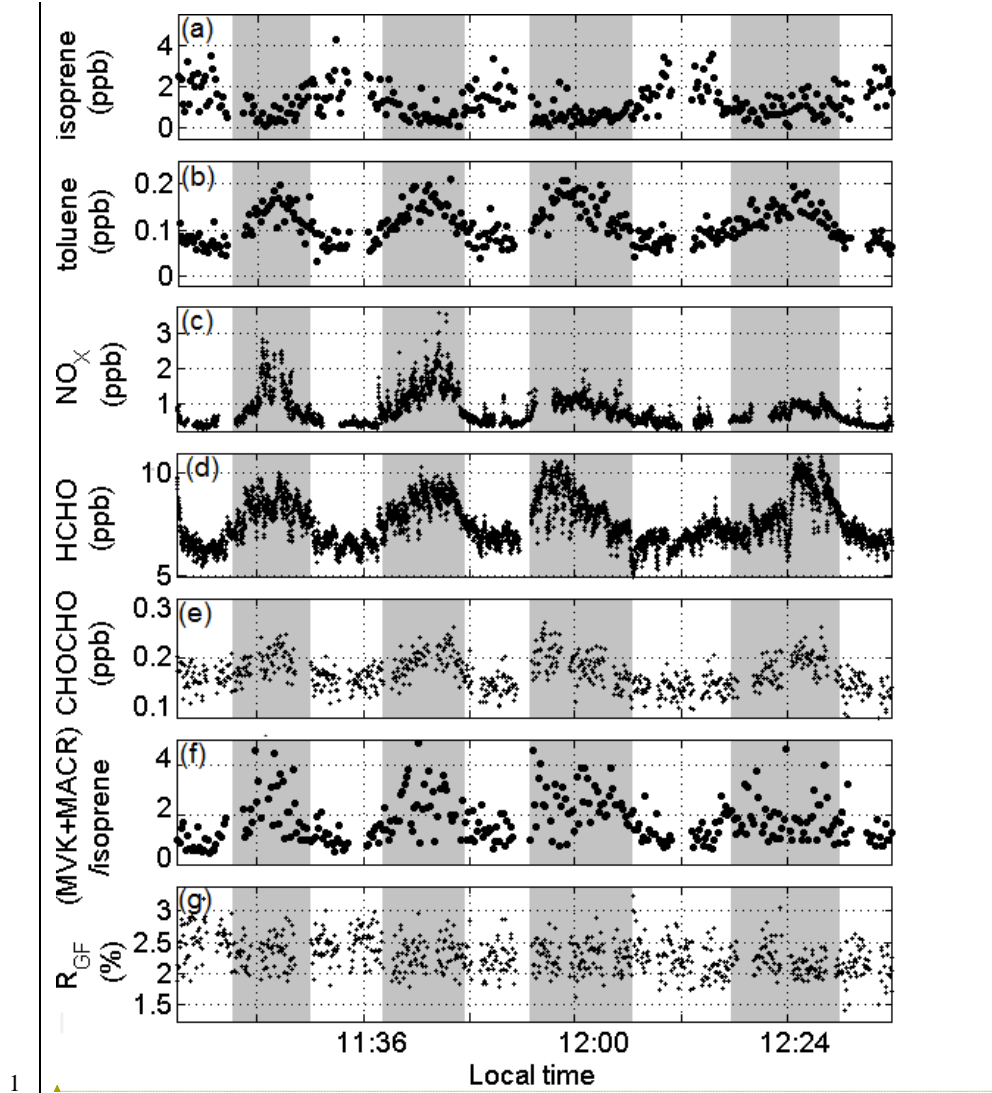
2

3 Figure 6. Flight track for 12 June 12, colored by CO, which shows the combined outflow of
 4 Atlanta, the airport, and a paper mill on the surrounding background. Measurements acquired in
 5 the shaded area are shown in Fig. 7.

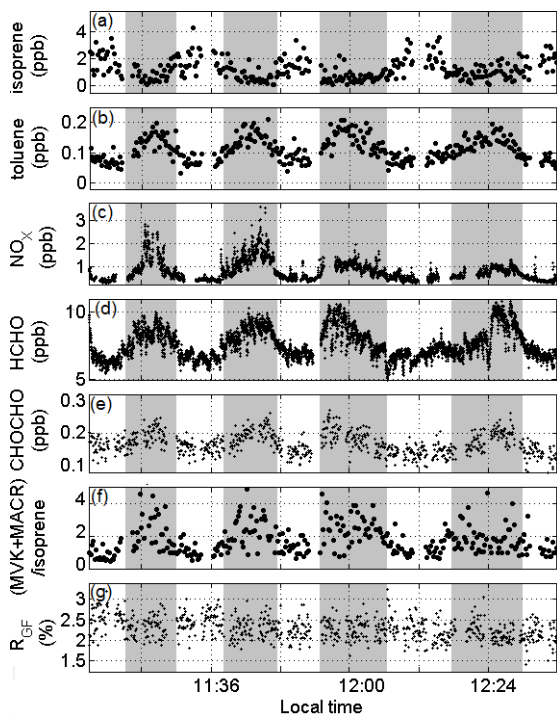
Formatted: Font color: Auto

Formatted: Font color: Auto

Formatted: Font color: Auto



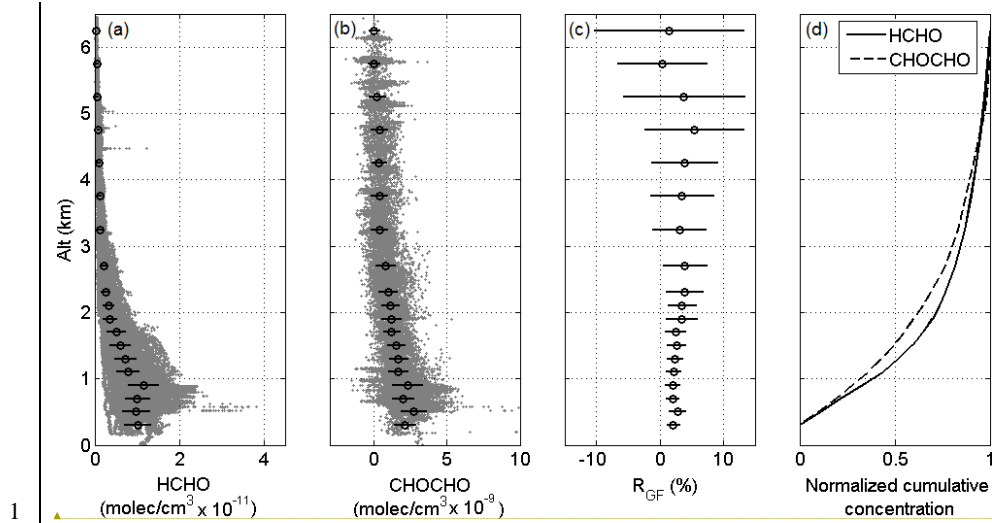
Formatted: Font color: Text 1



1

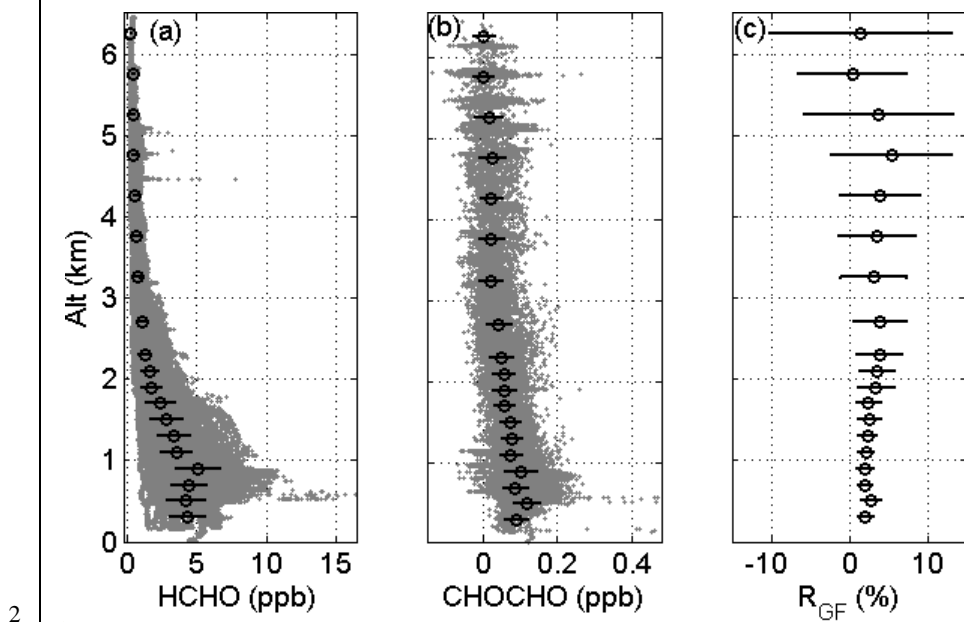
2 Figure 7. Measurements acquired on the 12 June 12th flight corresponding to the boxed in region
 3 in Fig. 6. Shaded regions indicate high anthropogenic influence. While the measurements alter
 4 between AVOC/high NO_x/NO_x and BVOC/low NO_x regimes, little change is seen in R_{GF} . The
 5 maximum values of NO_x/NO_x and (MVK+MACR)/isoprene fall above the limits shown here.

Formatted: Font color: Auto



1

Formatted: Font color: Text 1



2

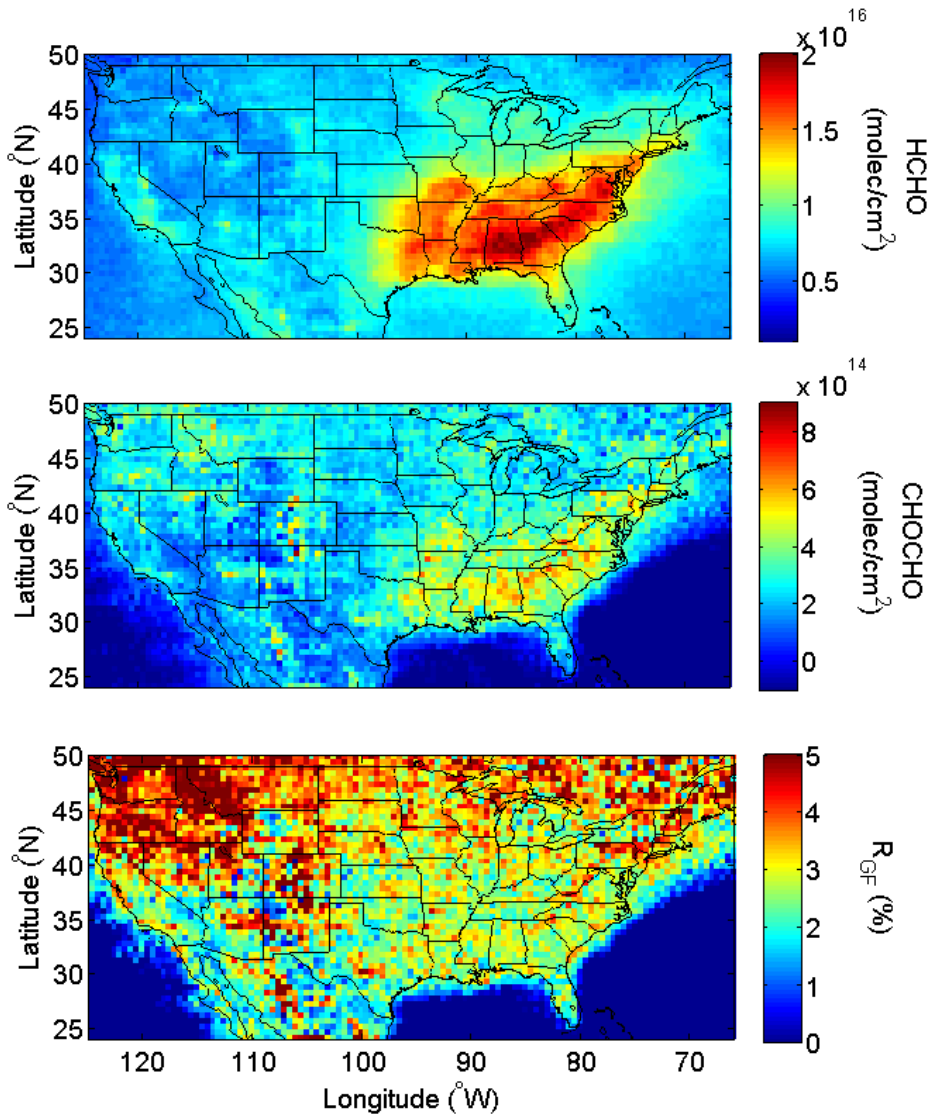
Formatted: Font color: Auto

3 Figure 8. Average vertical profile of (a) HCHO and (b) CHOCHO measurements acquired
 4 during the flights specified in Fig. 1. Gray dots represent all measurements, black circles are

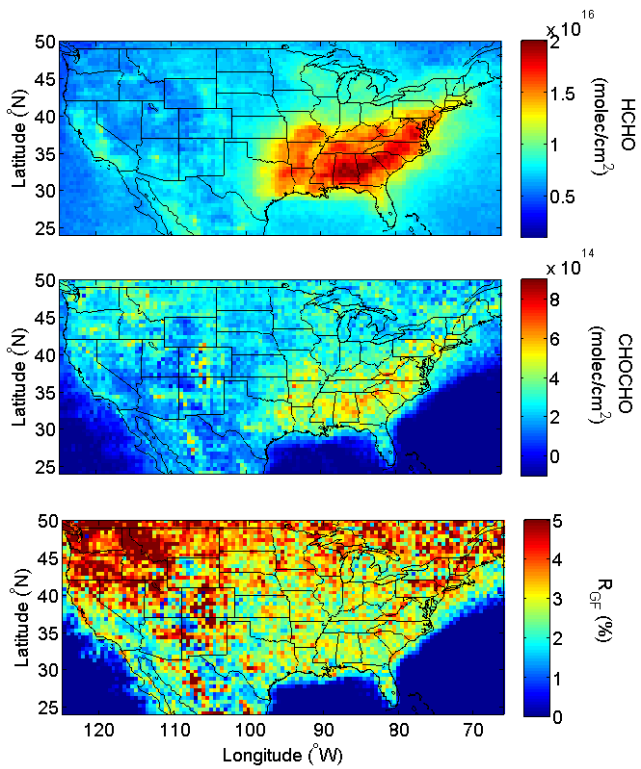
Formatted: Font color: Auto

1 averages in a given altitude bin, and error bars are standard deviation within that bin. Bins are
2 200 m in height from 200 to 2500 m, and 500 m thereafter. (c) R_{GF} calculated from average
3 ~~OVOC-HCHO and CHOCHO~~ profiles. Error bars are calculated from the standard deviations of
4 HCHO and CHOCHO observations. ~~(d) Cumulative concentration of HCHO and CHOCHO with~~
5 ~~altitude from 0.6 km, normalized to total column concentration.~~

Formatted: Font color: Auto



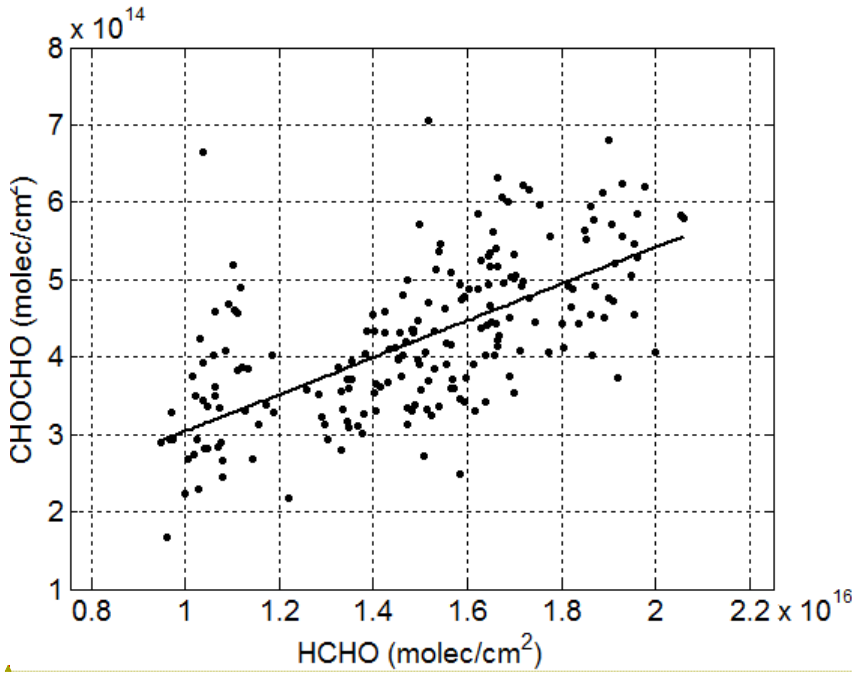
Formatted: Font color: Text 1



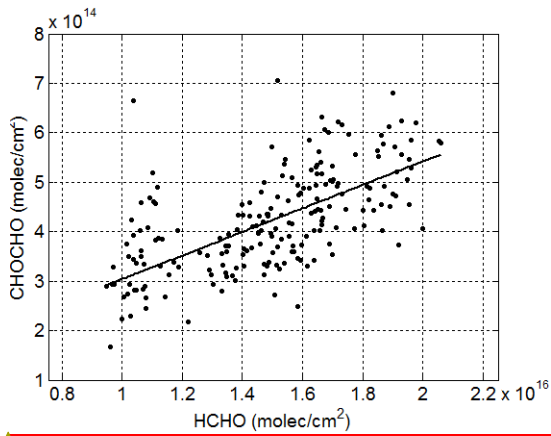
1
 2 Figure 9. OMI Satellite retrievals of HCHO and CHOCHO vertical density during June through
 3 August of 2007. The ratio to CHOCHO to HCHO is shown in the bottom panel.

Formatted: Font color: Auto

Formatted: Font color: Auto



Formatted: Font color: Text 1



Formatted: Font color: Auto

1

2

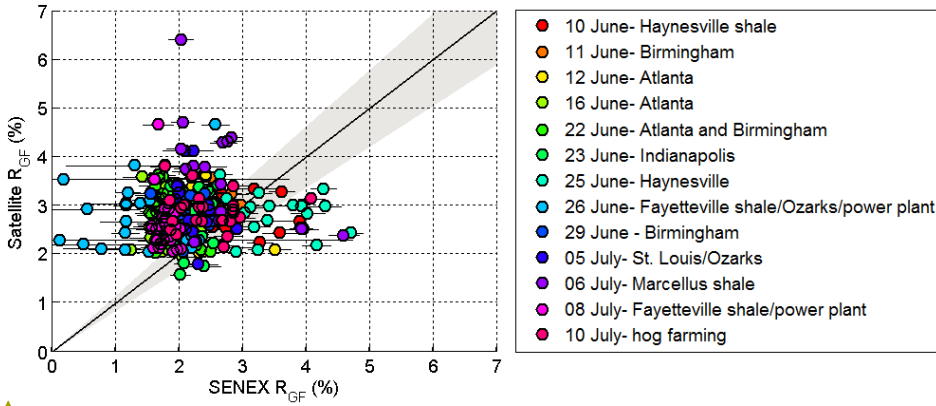
3 Figure 10. Satellite retrieval of CHOCHO v ~~HCHO~~HCHO corresponding to grid coordinates of

Formatted: Font color: Auto

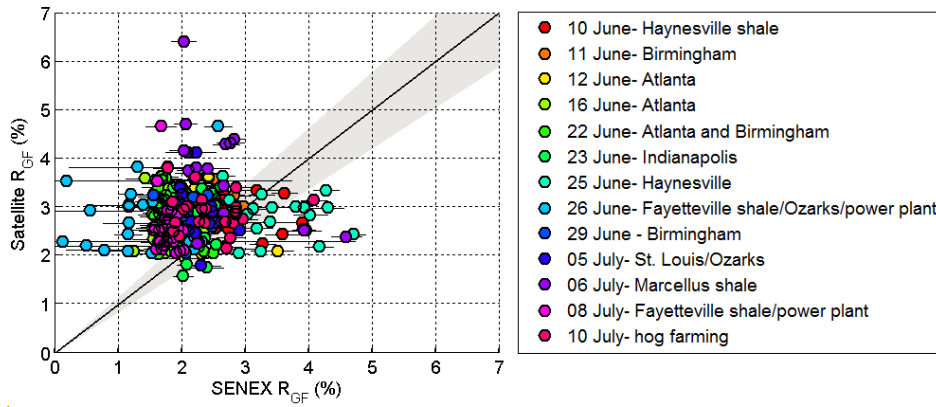
4 SENEX boundary layer measurements. Statistics for the linear fits are shown in Table 4.

Formatted: Font color: Auto

Formatted: Font color: Auto



Formatted: Font color: Text 1



Formatted: Font color: Auto

1

2

3 Figure 11. Satellite and SENEX R_{GF} . The line represents a 1-1 relationship, error bars represent
 4 standard deviations of SENEX measurements within the given pixel, and the shaded area
 5 represents the accuracy of the SENEX measurements.

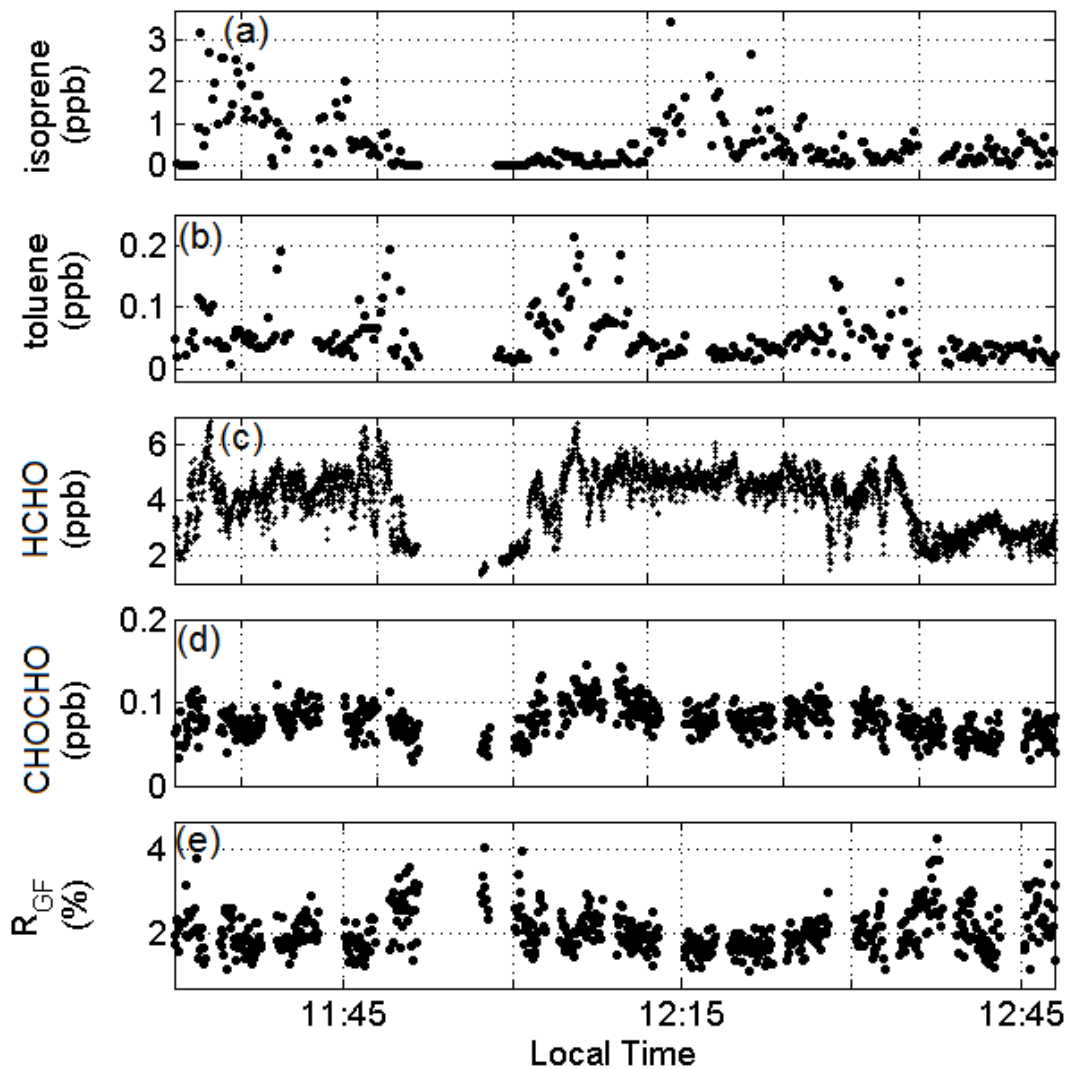
Formatted: Font color: Auto

1 This supporting information provides average flight conditions (Table S1), an additional
2 example in-and out of plume measurements of R_{GF} from the outflow of St. Louis (Fig. S1
3 and Fig. S2), as well as the individual vertical profile locations and measurements (Fig.
4 S3 and Fig. S4).
5

1 Table S1. Summary of meteorological conditions for flights used in the analysis of R_{GF} .

Flight date	Focal region	Time range (local)*	Average temperature (°C)
10 June 2014	Haynesville shale	11:21-15:08	25.2±1.3
11 June 2014	Birmingham	13:15-17:29	26.3±1.4
12 June 2014	Atlanta	09:51-15:26	25.8±1.3
16 June 2014	Atlanta	10:47-16:14	22.9±1.0
22 June 2014	Atlanta/Birmingham	10:37-16:39	22.3±1.4
23 June 2014	Indianapolis	10:50-13:20	22.9±0.8
25 June 2014	Haynesville shale	11:41-16:03	25.7±1.5
26 June 2014	Fayetteville shale/Ozarks	10:42-14:42	24.7±1.2
29 June 2014	Birmingham	12:21-16:55	24.2±1.0
05 July 2014	St. Louis/Ozarks	10:44-15:23	21.2±1.2
06 July 2014	Marcellus shale	11:11-14:09	21.4±0.7
08 July 2014	Fayetteville shale	10:59-16:07	25.4±1.9
10 July 2014	Hog farms	10:12-13:16	23.8±0.9

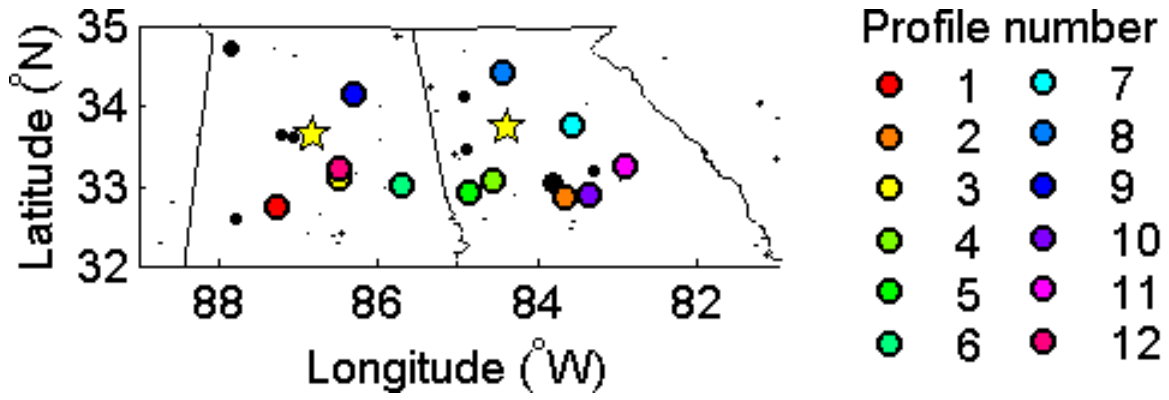
2 *Transit to and from region of flight's focus not included



1

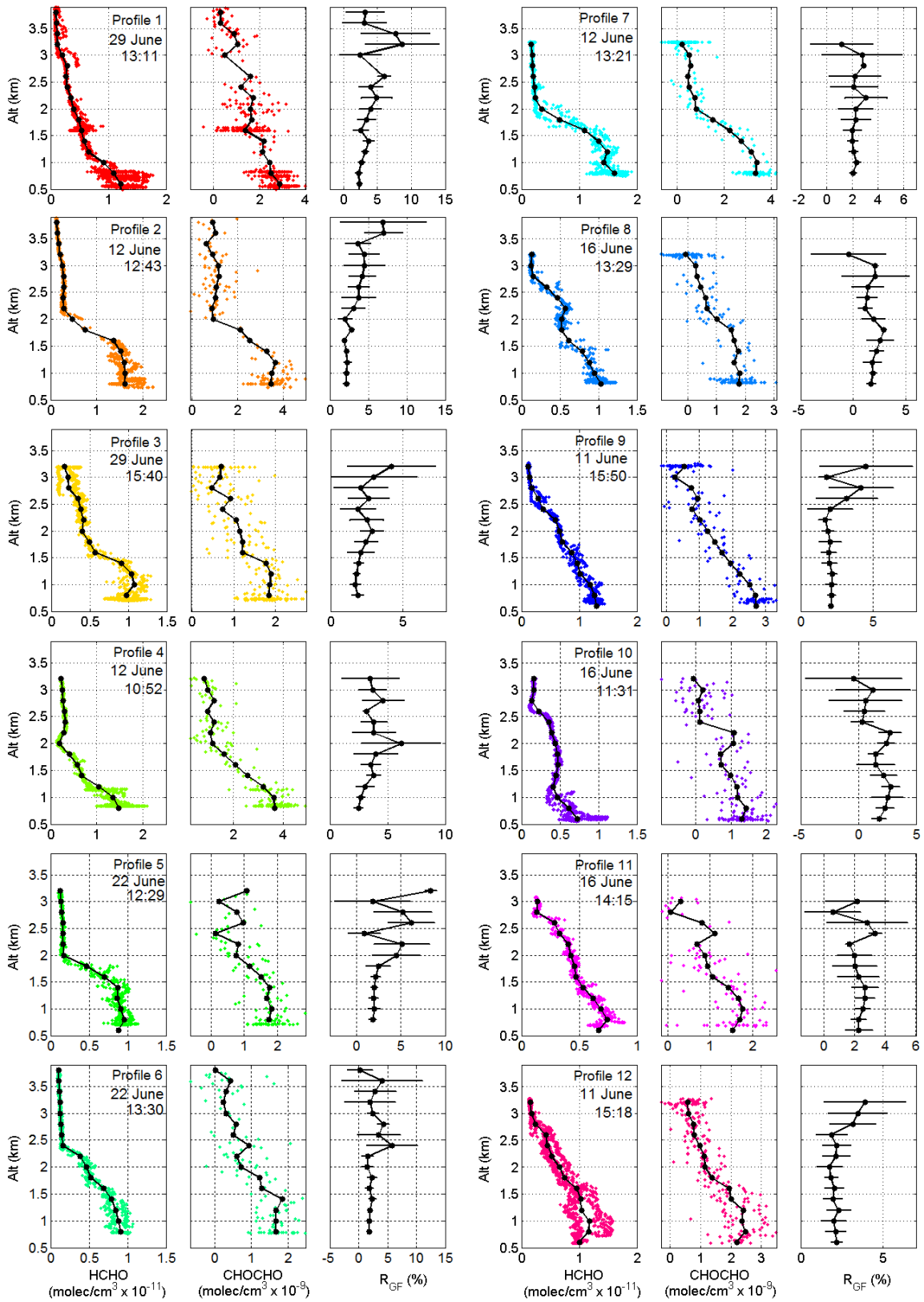
2 Figure S2. Measurements acquired on the July 5th flight corresponding to the boxed in
 3 region in Fig. S1. As in the June 12th flight near Atlanta, VOC speciation has little
 4 relationship with observed R_{GF} .

5



1

2 Figure S3. Locations of vertical profile measurements extending >3 km. Power plants
 3 markers are scaled by NO_x emissions.



1

1 Figure S4. Vertical profiles of HCHO and CHOCHO concentrations and R_{GF} at locations
2 shown in Fig. S3. Small markers indicate measurements, black circles represent the
3 average value in a 200 m altitude bin, and in the R_{GF} panels, error bars represent the
4 standard deviation of R_{GF} as calculated from the standard deviation of glyoxal and HCHO
5 in that altitude bin.